Dynamic Measurements on Electromagnetic Devices

By M. A. LOGAN

(Manuscript received July 6, 1953)

A sampling switch with adjustable make and fixed break times can be used to obtain dynamic measurements of reciprocating phenomena. A test set has been developed using this principle to measure the flux-time, current-time, displacement-time, and velocity-time response of electromagnets and similar devices. The tested device is steadily cycled. A dc instrument is switched in by the synchronous control at any preselected instant in the cycle, and out when a steady reference condition has been reached. The steady reading of the instrument is proportional to the value, at the closure instant, of the variable being measured. The instrument switching is controlled by an electronic timing system. This system operates mercury contact relays, which do the actual switching. For the displacement-time and velocity-time measurements, an optical transducer with associated dc amplifiers is added. The design of these devices is described. The results of an investigation of dynamic flux rise and decay in solid core electromagnets are reported. Modified first approximation equations are developed to give a better representation of eddy current effects.

Introduction

The application of common control methods to telephone switching systems has led to the widespread use of high-speed relays. The actuation time of these relays is affected by many parameters such as the power supplied, how far the armature has to move, the mechanical work the armature has to perform during its motion, the winding design, the magnetic structure, and eddy currents introduced in the magnetic members caused by the application of current to the winding. The eddy currents act to oppose a magnetic flux change and hence retard a building or decay of flux. This causes the actuation time to be increased compared to a relay without such effects. An analytical determination of the development and effects of eddy currents can be made for simple sym-

metrical magnetic structures having an infinitely long or torus shaped round or rectangular cross-section, assuming linear magnetization characteristics. However, for relay-like structures having air gaps, leakage flux which only partly completes its circuit through the magnetic material, varying cross-section so that boundary conditions become complicated, and non-linear magnetic properties, an analytical approach becomes unmanageable.

For a fundamental study and direct measurement of eddy current effects, a test set has been developed to measure the dynamic flux rise and decay characteristics of relays, and similar structures. This test set is electronically operated on a synchronous switching principle. It displays on an ordinary dc instrument, as a steady reading, the instantaneous flux obtaining at any selected time after energization or de-energization of the magnet.

The application of the test set is restricted to devices which operate under conditions of suddenly applied or removed dc voltage and which can be cycled between these two conditions until the dc instrument reaches its steady state reading.

This article will present the theory of the basic synchronous switching circuit and the relation applying between the dc instrument reading and the instantaneous flux linkages, a description of the electronic control circuits, and measurements of dynamic flux rise and decay using solid core electromagnets.

Supplementary additions to the basic circuit are available using the same principles, to measure current-time, displacement-time, and velocity-time curves of reciprocating devices. The first fundamental measuring set using the switching principle, was built by E. L. Norton[1] in 1938. The earlier set used a synchronous, motor driven, phase adjustable commutator, to perform the switching. A limitation of the earlier set in how fast it could be operated, combined with brush wear and chatter troubles led to the development of the new electronically controlled set employing sealed mercury contact relays to perform the switching.

Part I — Description of Fluxmeter System

BASIC MEASURING CIRCUIT

A schematic of the basic measuring circuit is shown in Fig. 1. A battery switching contact indicated as A, applies and removes voltage to the magnetizing winding of the electromagnetic device under test with a 50 per cent duty cycle. The time of one complete cycle is indicated as T. The electromagnetic device is equipped with a search coil of N turns, having dc resistance, including wiring, of R_c ohms. A B contact, synchronously switched at instants to be described later, connects a dc microammeter to the search coil. A damping contact C connects the instrument to a resistance, preset to the same value as the search coil, when the instrument is not connected to the latter, thus providing the same instrument damping at all times.

The A timing cycle is shown schematically for one interval T. Next below is shown the cycle for the B contact, followed by that for the C contact. The B contact always opens and the C contact closes just before the A contact closes. The point of closure of the B contact, indicated as t_1 may be adjusted to occur at any time during the cycle T. The cycle time T is chosen sufficiently long so that the flux in the electromagnet has sufficient time to reach a substantially steady state during both the closed and the open intervals.

The flux rise and decay have the general characteristics shown as the φ curve, while below it is the induced voltage in the search coil, exactly given by Lenz's Law

$$e = N\frac{d\varphi}{dt}. \tag{1}$$

The first property of this last curve to observe is that the positive and negative areas are exactly equal. Otherwise a dc instrument connected permanently to the search coil would show a dc current flow. The second property is that the area of the curve up to some time t_1 is proportional to the instantaneous flux at the time t_1. Finally, this unshaded area is numerically equal but opposite in sign to the shaded remainder of the area, taking into account the signs of the two components of the remainder. The operation of the test set depends upon measuring this shaded area.

Let the flux linking the search coil of N turns at any time be φ. Assume that the microammeter has a resistance R_m and inductance L_m. The current flowing in the meter mesh while the B contact is closed is

$$N\frac{d\varphi}{dt} + L_m\frac{di}{dt} + (R_m + R_c)i = 0. \tag{2}$$

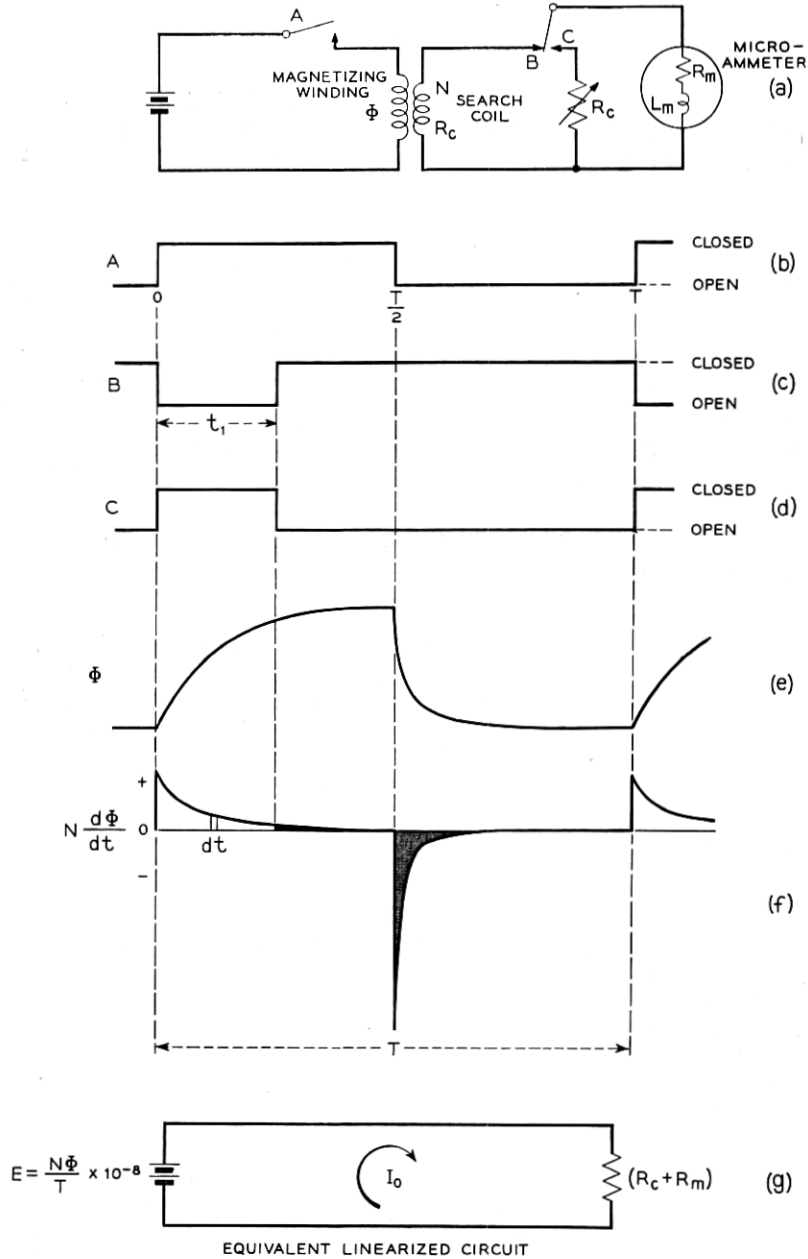

Fig. 1 — Fundamental operation of dynamic measuring set.

The dc instrument will read the average value of current for the cycle. As the period of the cycle is T, and t_1 is the chosen delay for closure of the B contact measured from the time of the A closure, the direct current indicated by the instrument will be:

$$I_0 = \frac{1}{T}\int_{t_1}^{T} i\,dt = -\frac{1}{(R_m + R_c)T}\int_{t_1}^{T}\frac{d}{dt}(N\varphi + L_m i)\,dt = \frac{(N\varphi + L_m i)_{t_1} - (N\varphi + L_m i)_T}{(R_m + R_c)T}. \tag{3}$$

Now the product $L_m i$ at t_1 when the B contact is closed must be zero. Furthermore, if the period T is long in comparison with the time of rise and decay of the flux, and with the time constant L/R of the measuring circuit, the product $L_m i$ is also negligible at $t = T$. We then have:

$$\Phi_{t_1} - \Phi_T = \frac{RTI_0}{N} \times 10^8 \text{ Maxwells}, \tag{4}$$

where R is now the total resistance of the measuring circuit. The factor 10^8 has been added to convert from practical units to c.g.s. units. The flux Φ_T is the residual flux, so that if this is taken as a reference value, the value of the flux at the time of closing the B contact is simply

$$\Phi = \frac{RTI_0}{N} \times 10^8 \text{ Maxwells}. \tag{5}$$

It may be objected that the flux in equation (2) is made up not only of the flux to be measured but also of a component due to the current in the measuring circuit. This is true, and the flux linking the search coil changes differently during the time the B contact is closed compared to that without the instrument circuit. Note, however, that we are not concerned with how the flux varies between the times t_1 and T but only with its value at the limits. Since the flux at t_1 is that which has been established with the search coil circuit open, the one requirement is that the constants be such that the current in the measuring circuit be substantially zero just before T. This can be verified through the measurements themselves by noting whether there is any change in measured flux in this interval. If there is, then the cycle time T can be increased until this requirement is met.

It will be convenient later to regard the switched meter as a linearized circuit composed of an equivalent dc voltage

$$E = \frac{N\Phi}{T} \times 10^{-8} \text{ volts} \tag{6}$$

in series with the resistor R, causing a dc current I_0 to flow, Fig. 1 (g).

MEASUREMENT OF CURRENT

The instantaneous value of current in a circuit being cycled by the A contact is measured by inserting the primary of a toroidal air core transformer in series with the circuit as shown in Fig. 2. The secondary is connected to the meter through the B contact. The best design consists of a secondary occupying half the winding volume and wound to the same resistance as the meter. The primary can be wound in two sections, half inside and half outside of the secondary to provide maximum mutual inductance, of a wire coarse enough to provide the number of turns for a convenient meter deflection. In an air core transformer, the magnetic circuit is linear and the flux exactly proportional to the current, a situation that does not exist when magnetic materials are present. Because of this linearity, the analysis can be made in terms of inductances and currents rather than flux linkages and currents.

By definition, the voltage induced in the secondary of a linear transformer is related to the primary current, through the mutual inductance M by the relation:

$$e = M \frac{di}{dt}, \tag{7}$$

which corresponds exactly to (1) with M substituted for N, and i for φ. Hence, the instantaneous current at time t_1 is given by the relation

$$i = \frac{RTI_0}{M}, \tag{8}$$

where the other symbols have the same significance as before. This relationship makes the calibration of the mutual inductance easy by setting up a battery and resistor for the primary circuit and measuring the steady state current with an ammeter. Then when the A contact is being switched and the instrument current I_0 is read, corresponding to the known final primary current i, relation (8) can be solved for M.

MEASUREMENT OF FLUX USING A BRIDGE CIRCUIT

The search coil method of measurement just described is preferred because of the absence of any dc voltage in the meter circuit. However,

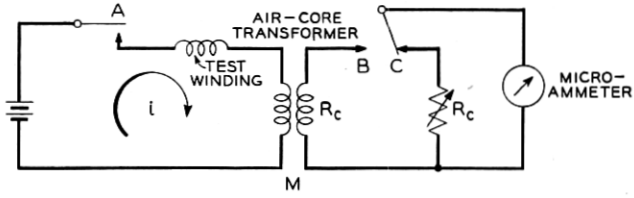

Fig. 2 — Circuit for the measurement of current.

sometimes the use of a search coil is inconvenient, or for other reasons it is desired to measure the flux linkages in the magnetizing winding itself. The test set includes a bridge circuit shown in Fig. 3 for such measurements. With the contacts A and B closed and the bridge in the flux rise arrangement, the bridge is first balanced for no current in the instrument, by adjustment of R_d. The same instrument is used for setting the balance as later used for the flux measurement. The damping resistance is next set to the value facing the instrument, namely,

$$R_c = \frac{K}{K+1}(R_0 + R_d). \tag{9}$$

If then the contacts are operated with the period T, the instrument will read a current I_0, and the flux-turns at time t_1 during rise will be

$$N\Phi \times 10^{-8} = R_m I_0 T\left[1 + K\left(1 + \frac{R_0}{R_m} + \frac{R_d}{R_m}\right)\right] - L_1 i, \tag{10}$$

where N is the number of turns of the winding, Φ is the average flux per turn, and the other quantities are indicated on the drawing. The term $L_1 i$ is a correction term, usually negligible, involving the self inductance of the primary of the air core current transformer and i the instantaneous

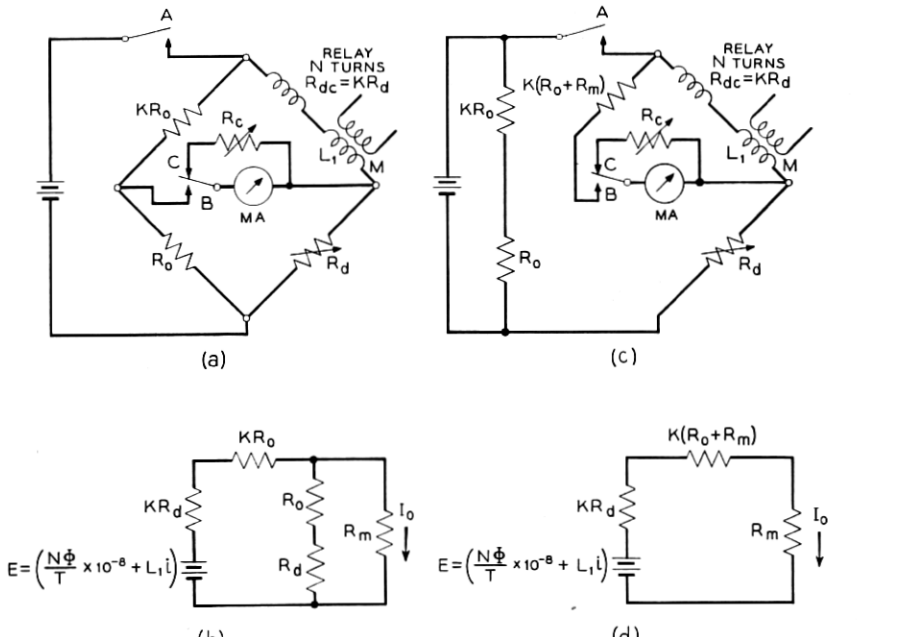

Fig. 3 — Bridge circuit for the measurement of flux — (a) and (b), rise; (c) and (d), decay.

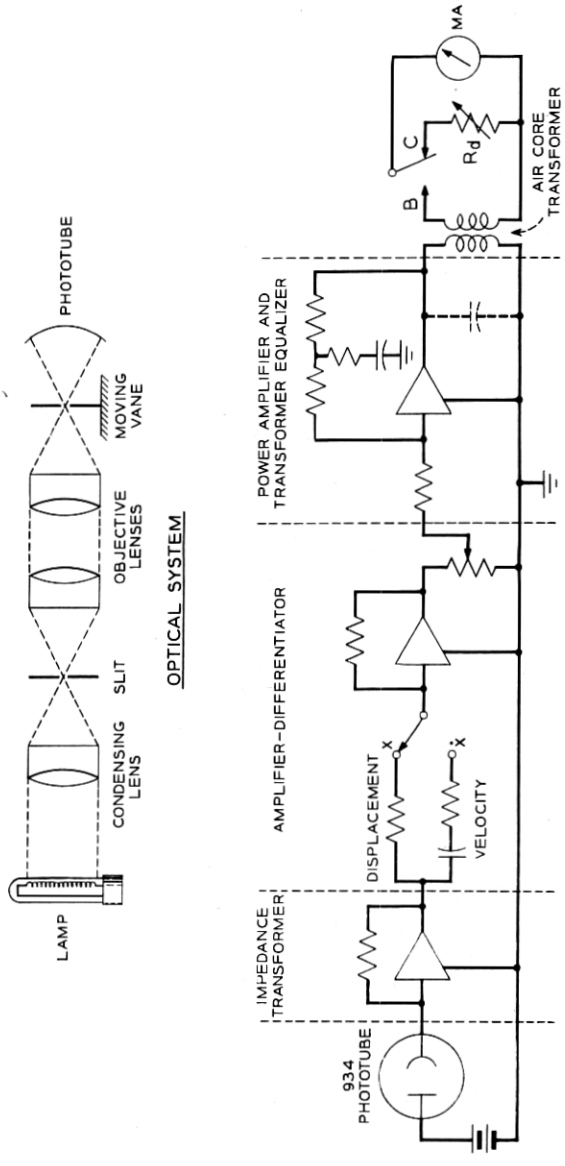

Fig. 4 — Block diagram of photocell amplifier system.

current at the time t_1; i is determined by a separate measurement described above. If its value is not needed, the air core coil can be omitted from the circuit.

For flux decay measurements made after the A contact has opened, the bridge circuit has to be modified to remove the resistance R_0 and KR_0 from being across the electromagnet and affecting its flux decay. They are transferred to the battery side of the A contact as shown in Fig. 3(c), to maintain the same battery drain. This avoids any error due to the internal resistance of the battery, which would otherwise cause the final flux at the end of a rise test to differ from the initial flux at the beginning of a decay test. The added resistor $K(R_0 + R_m)$ is connected in series with the meter to make the expression for the flux-turn linkages the same as before. For decay measurements the damping resistor is set at the value

$$R_c = K(R_0 + R_m + R_d). \tag{11}$$

In Figs. 3(b) and 3(d) are shown the linearized equivalent circuits for rise and decay respectively, from which equation (10) above can be derived conveniently.

MEASUREMENT OF DISPLACEMENT AND VELOCITY

An optical probe is provided, in which the amount of light falling on a photocell is controlled by the relative position of two flags, one cemented on each of the relatively moving parts to be studied, such as an electromagnet. The change in output current from the photocell thus is proportional to the displacement of the armature with respect to the core, one flag being on each. A block diagram of the system is shown in Fig. 4. Amplifiers effective from dc up to a frequency determined by the resolution required, with substantially no phase shift, deliver a current into the primary of an air core transformer proportional to the instantaneous displacement of the armature. By virtue of the linearity of this transformer, the flux developed is proportional to the displacement. Thus by operating the electromagnet with the A contact and connecting the secondary of the transformer to the B contact, the instrument gives a dc reading proportional to the armature displacement at the time the B contact closes. The total displacement can be measured statically. The instrument reading at a time after complete operation corresponds to this known displacement, permitting the scale to be converted to a displacement scale.

By changing one amplifier input resistor to a capacitor, the amplifier

becomes a differentiator, in which the output current is proportional to rate of change of input voltage. With this one change, the instrument reads the instantaneous velocity of the armature. Under these conditions, the second amplifier differentiates the input voltage once, the output transformer differentiates a second time, and the dc instrument integrates once, leaving a net result of one differentiation.

Description of System Components

FLUXMETER

General

In the following descriptions of the several components of the system, the general characteristics required are considered, the specific deviations from ideal are determined, and an evaluation of the measurement errors is made. The description starts with the dc instrument followed by the associated vacuum tube filter. Then the heart of the system, the contact switching circuit itself is considered. Following this is the timing impulse generating circuit, the counting rings, the time selector, coincidence circuits, memory, and relay control circuits. These elements make up the fluxmeter proper.

The auxiliary circuits for displacement-time and velocity-time measurements are the concern of the next part of the paper. The components are the optical system, the photocell amplifier, the amplifier-differentiator and finally the output amplifier.

The last section first shows typical measurements on a telephone type relay. Then a description of a more fundamental study of dynamic flux rise and decay in solid core electromagnets is given. This study has led to two new first approximation equations for dynamic flux rise and decay, as will be seen.

Dc Instrument and Effect of Damping Resistance

The dc instrument used for a majority of the measurements is a heavily damped 50.0-ohm, 200-microampere full scale instrument, with a ½ per cent of full scale accuracy. The open circuit decay time constant is about 2 seconds, and with a shorted winding about 4 seconds. On Fig. 5 is shown a plot of the decay time constant referred to a short circuit, versus the damping resistance referred to the meter resistance.

An evaluation of the small error introduced by not providing the damping resistor is as follows. Consider a square wave flux pattern produced by an ideal electromagnet, with zero winding time constant or

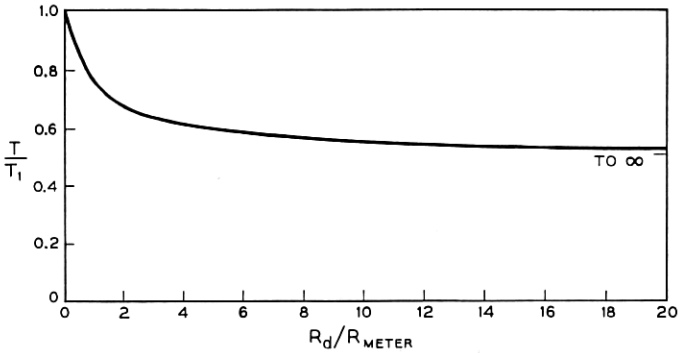

Fig. 5 — Decay time constant of DC instrument.

eddy currents. The induced voltage in the search coil then consists of two equal and opposite impulses occurring respectively at 0 and T/2. To measure the constant flux, the switching epoch can be anywhere between these two values. The switching omits the impulse at zero time. For limiting cases t_1 can approach either 0 or T/2. The instrument reading of course should be independent of the choice, as the flux remains at the constant maximum throughout this interval. The instrument receives only the decay impulse, and thus there will be an average dc component.

For the case of t_1 approaching zero, the instrument is always connected to the search coil, which usually is of negligible resistance and the short circuit meter decay time constant applies. Just before a succeeding impulse, the meter will have decayed to a relative value of:

$$e^{-T/T_1} \approx 1 - \frac{T}{T_1}, \tag{12}$$

where T is the cycle time as before and T_1 is the short circuit decay time constant. The pointer next abruptly rises to its original maximum value, followed again by another equal decay in a cyclic manner.

For the case of t_1 approaching T/2, the instrument is connected to the the search coil only half the time, being open circuited for the remainder of the time, if no damping resistor is provided. It thus decays at two different rates following the impulse. The first half is the same as before but the second half is under the condition of open circuit. For small errors the relative decay will be:

$$e^{-T/2T_1} e^{-T/2T_2} \approx 1 - \frac{T}{2}\left[\frac{1}{T_1} + \frac{1}{T_2}\right], \tag{13}$$

where T_2 is the open circuit decay time constant.

The search coil impulse is the same in each case, and for small errors, the instrument will rise the same amount for either condition followed by equal decays. The two maximum values M_1 and M_2 are not equal but are related by:

$$M_1 \frac{T}{T_1} \approx M_2 \frac{T}{2}\left(\frac{1}{T_1} + \frac{1}{T_2}\right) \tag{14}$$

$$\frac{M_1}{M_2} \approx \frac{1}{2}\left(1 + \frac{T_1}{T_2}\right) \tag{15}$$

The ratio of the two instrument readings thus is a function of the ratio of the two instrument decay time constants. For the case of $T_1 = 4$ sec., $T_2 = 2$ sec., the limiting error is 33 per cent. This shows that without a damping resistor, the error can be many times the ½ per cent instrument error, but that the timing for switching the meter damping is not critical. That is, small time gaps with the damper off will introduce an insignificant error. In a sense, the omission of the damper is equivalent to using an electronic integrator with finite internal gain.

Vacuum Tube Filter Circuit[1]

The above discussion brings out the fact that visible motion of th instrument pointer without a filter occurs, increasing as the cycle time ie lengthened. From equation (12) and using $T = 0.1$ sec., and $T_1 = 4$ sec.s the amplitude would be about 2½ per cent of full scale. Reading the center of the vibration is easy for cycle times T less than 0.1 second and for such measurements the filter is not used. Many measurements, however, require a slow pulse rate and even a sluggish instrument will follow the pulses to such an extent that an accurate reading is impossible.

Fig. 6 is a schematic of a vacuum tube circuit which serves as a very efficient low pass filter. This filter must fulfill a variety of very stringent requirements, chief of which may be listed:

(a) Low loss to direct current.

(b) High loss, probably exceeding 30 db to frequencies above one cycle per second.

(c) A constant resistance input.

(d) Ability to suppress peaks of relatively high voltage of the order of several hundred or thousand times the dc voltage being measured.

(e) No effect other than one which may be accurately calculated on the dc reading.

(f) The circuit should not greatly increase the time required for the instrument to reach a steady reading.

Requirement (c) may call for some comment. It was pointed out earlier that the method requires the time constant of the measuring circuit to be small in comparison with the period of the pulses. A filter built in the ordinary way to have high suppression to pulses of period T would not have a time constant small in comparison with this figure. The require-

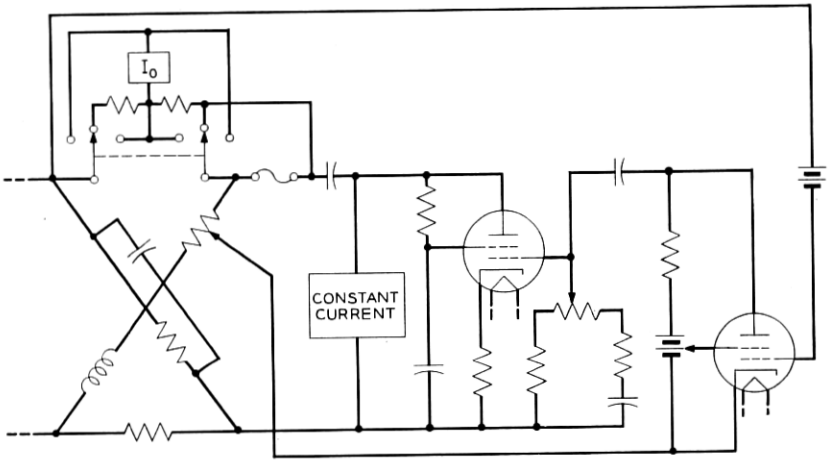

Fig. 6 — Vacuum tube low pass filter circuit.

ment of constant resistance input is a convenient way of expressing the necessity of fulfilling this condition.

The original work on the system used was done by R. F. Wick, and the features to be described are due to him and E. L. Norton. From left to right in Fig. 6, the elements are as follows: a balanced impedance bridge containing the ammeter in one arm, a blocking condenser, a constant current high impedance power supply for the power tube, and a two stage amplifier with an interstage phase adjusting circuit. The three-point double-pole key when in the normal position removes the meter (50 ohms) and substitutes a 50-ohm resistor. When off-normal, the meter is connected in either polarity.

The operation of the circuit is best understood by assuming the reactance elements to be omitted from the bridge and the contact on the potentiometer forming one diagonal to be at the lower left. The input to the amplifier is then directly across the line and any feedback is elimi-

nated, since the bridge is balanced. Any alternating component applied will be amplified and sent back through the meter in the opposite polarity to that coming directly from the line. If then the gain in the amplifier is correct and its phase shift nearly zero, the alternating component through the meter will be greatly reduced.

The bridge provides the constant resistance feature at the input, since the output of the amplifier can have no effect on the input impedance. It does however necessitate a loss from both line and amplifier to the measuring instrument.

Practically, the difficulty in design is in securing an amplifier with enough peak output capacity and negligible phase shift at frequencies from one cycle up. This has been accomplished by several methods. Most of the phase shift is introduced by the plate condenser in the last stage. The effect of this is reduced by the constant current power supply.

The gain of the amplifier is controlled by feedback secured by the potentiometer in the diagonal arm of the bridge. The gain is sufficient so that a substantial amount of feedback may be used with a consequent further reduction in phase shift.

The final phase compensation is secured by the interstage potentiometer. The effect of this is illustrated in Fig. 7. The lower curve is the net phase shift of the amplifier without the interstage circuit. The upper curve is the phase shift which may be introduced at the grid of the second stage. By proper adjustment, these may be made to compensate each other down to a frequency of one or two cycles. The circuit constants are such that the final adjustment of low frequency phase may be made with a negligible effect on high-frequency gain. It may be of interest that if the bridge is unbalanced by shorting the lower 50-ohm resistance, an error of 20 per cent or more is introduced in the dc reading due to the extremely large effective reactance of the feedback amplifier. If the bridge is unbalanced by shorting the instrument the amplifier is quite likely to "motor-boat" and blow the fuse used for protection. It is for this reason that the instrument key may be set to replace the instrument by a 50-ohm resistor. When in this position the fuse is also shorted to avoid needlessly blowing it due to the high surges which frequently occur when the amplifier is turned on and the condensers start to charge.

The filter as described, omitting the reactance elements from the bridge, would be entirely satisfactory within the power capacity of the amplifier. With certain measurements, notably those of velocity, the peaks of the wave as applied to the filter, which in this case would be proportional to acceleration, are so high that no reasonable amplifier would be able to handle them. These knifelike peaks however are so sharp that they may

easily be removed by reactance elements added to the bridge as shown. It will be noted that the bridge is still of constant resistance, and is still balanced at all frequencies.

Three adjustments are provided on the amplifier: one controls the feedback, a second the phase correction, and the third the plate current. The amount of suppression is controlled by a three position key which may be used to cut down the sizes of the capacitors in the circuit in a ratio of two and four to one. In cases where one of the higher pulse rates is used, adequate suppression and somewhat faster readings may be secured by using smaller capacitors. With the maximum suppression, two cycles may be reduced to such an extent that it has no detectable

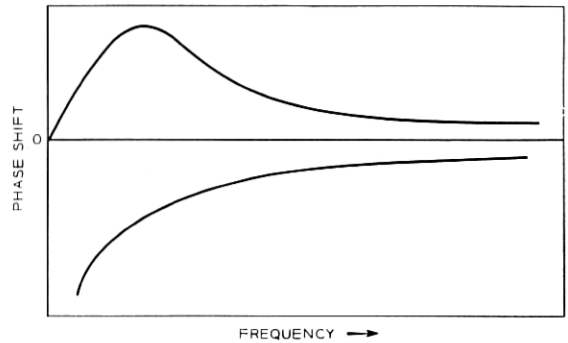

Fig. 7 — Illustration of method for phase compensation of amplifier.

effect on the meter pointer. Accurate measurements at one cycle may be made, although there is a slight motion of the pointer.

Analytical studies have indicated that the transient response of the circuit depends to a large extent on the ratio of the interstage coupling capacitor to the output capacitor and moreover that there is an optimum ratio of the phase compensating capacitor to the other two. In altering the amount of suppression therefore, the ratios of the three capacitors are held constant.

The Switching Circuit

Requirements. The basic feature of this measuring system is the switching circuit, consisting of the A, B and C contacts. The requirements for these contacts are: (a) Negligible dc resistance, (b) No contact chatter, (c) Contact potential less than 10 microvolts, and (d) Stability of operation of 20 microseconds. Consideration of these facters led to the selection of mercury contact relays as the basic switching elements. The choice

of relays leads to additional requirements: (e) Substantially equal operate and release times, (f) A make and a break contact, and (g) Substantially zero transfer or bridging time when operated or released.

The first requirement is to avoid correction terms in the test set equations. The second is to make the test set operation conform to the differential equation applying. The third depends upon the fact that meters having dc resistances of the order of 50 ohms are used, and no error deflection due to contact potential effects should be present. The stability requirement results from an objective of studying flux phenomena in intervals as small as 25 microseconds. The added relay requirements will be developed during the switching circuit description. All except the last can be met by individual relays. The last one has not been met by individual relays, but by using contacts of two relays actuated simultaneously, and adjusting their relative timing by winding shunts, the contact switching interval can be reduced to a few microseconds.

Contact Operation. The switching functions required were shown in Figs. 1 (b), (c) and (d) where the interval t_1 can be as low as 25 microseconds or almost as long as T. The A switch in unaffected in duty cycle, but the B and C switches vary from 0 to 100 per cent duty cycle. The operate and release times of relays are affected by their duty cycle and for low or high values become very erratic. To avoid this effect all relays are operated with a 50 per cent duty cycle, and the switching is accomplished by combinations of relay contacts. The epoch of the B relay cycle can be adjusted by manual selection, anywhere between 0 and $T/2$. This is shown schematically in Fig. 8 for the make contacts. The break contacts of course show exactly the reverse behavior. The C make contact is fixed in phase and is set to open just before the A contact closes.

To produce a B cycle for flux rise shown in Fig. 1 (c) where t_1 is less than $T/2$, a parallel connection of the B and C make contacts is used. To pro-

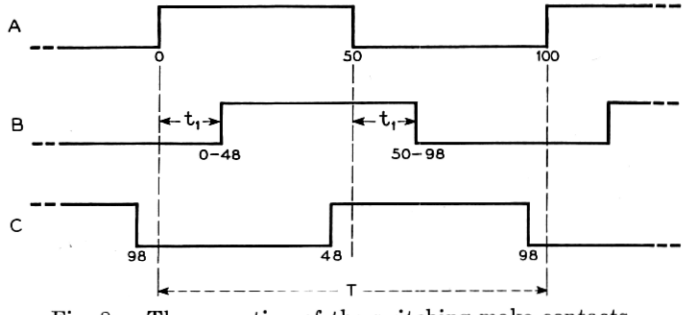

Fig. 8 — The operation of the switching make contacts.

duce a B cycle for flux decay where t_1 is greater than $T/2$, a break contact on the B relay is used in series with the C make contact. Note that in all conditions the meter circuit closure is performed by a B contact and the meter circuit open is performed by the C contact, in fixed phase relationship to the A contact. The addition of the switched meter damping resistor is accomplished by other contacts on the same relays.

A minimum contact circuit[2] to perform all these switchings is shown in Fig. 9 but was found to be unsatisfactory because of failure to meet requirement (g) above. Only a single transfer switch is necessary to change from flux rise to decay, by transferring the wire marked "x" from the search coil to the damping resistance.

The relays are shown in the released position with the break contacts closed. For the flux rise circuit, contact B can have a momentary open interval when it operates. However, it must not bridge or the damping resistor will momentarily be across the instrument at the initial connection, causing an error. But after contact C operates and then B releases at $(T/2 + t_1)$, an open interval at B will momentarily disconnect the instrument. This would cut out part of the current which must be integrated, causing an error. Thus there are conflicting requirements for flux rise measurements, and transfer contacts of a single relay cannot meet both simultaneously. For flux decay, the B contact cannot bridge because when it releases to connect the instrument, a bridging would momentarily connect the damping resistor across the instrument at the instant of greatest interest, causing an error. The requirements for the C contact are of the same type but less stringent, as the flux is never changing rapidly whenever it is switched.

The foregoing discussion was directed toward establishing the basis for the requirements (f) and (g) above. The former is because of the need for phase reversals in contact operation to perform the necessary

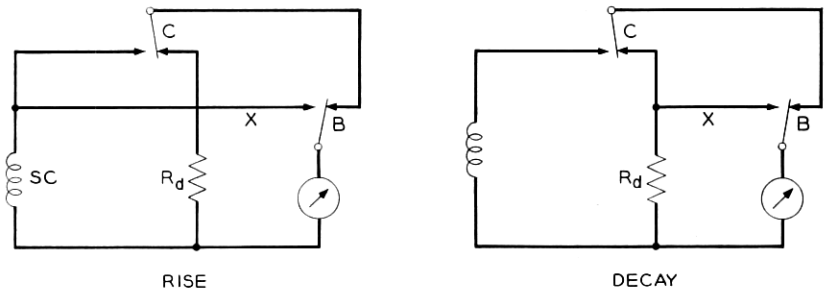

Fig. 9 — Unsatisfactory minimum contact circuit because of transit time requirements.

instrument and damping resistor switching. The latter is to eliminate errors due to momentary circuit configurations not in accordance with the basic equation (3).

The final circuit developed is shown in Fig. 10, which uses two B relays, called $B1$ and $B2$, a single C relay, and compatible timing requirements for the two B relays whose windings are connected in series. In all cases $B1$ shall be faster than $B2$. The former controls the damping resistor while the latter switches the instrument. A composite circuit is drawn, with the cross marks indicating a closed contact for the function being measured, open otherwise. The change from rise to decay in this circuit requires four switch contacts compared to two for the minimum contact circuit. As before, the relay contacts are all shown in the unoperated position. A preliminary sorting of the $B1$ and $B2$ relays is required and is based on operate and release time measurements. The faster relay is assigned as $B1$, the other as $B2$. $B2$ is further slowed down selectively to match the A relay as to operate and release time by the shunts and diode shown in Fig. 10.

$B2$ can be lined up with the A contact both for simultaneous closure of the make contacts when $t_1 = 0$ and for simultaneous closure of the

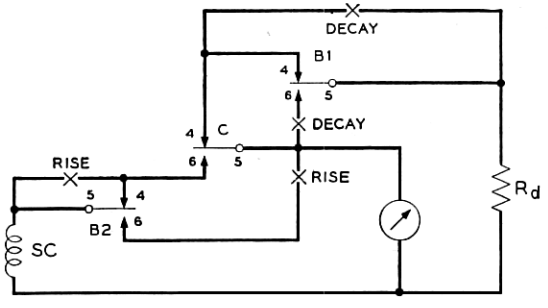

(a)

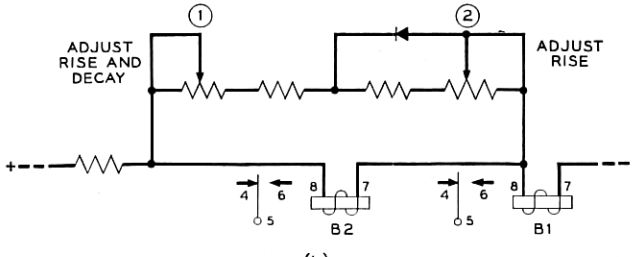

(b)

Fig. 10 — Final schematic of basic contact circuit.

break contact of $B1$ with the opening of the make contact of A. The A relay winding has a somewhat similar but fixed set of shunts across it, to slow it down with respect to $B2$ and to equalize operate and release time. The adjustment of the two potentiometers proceeds as follows. The time t_1 is set at 0, flux decay is chosen, and potentiometer 1 is adjusted to the point where the meter just starts to drop from the full reading. Then flux rise is chosen and the potentiometer 2 is adjusted to the point where the meter just starts to rise from zero. A fine check on these settings is to record the meter readings for a few equal small time steps and observe that the successive differences are consistent.

For applying an on and off battery condition as shown in Fig. 9 for the A contact, only one contact on one relay is used. The A contact circuit actually is made of two pairs of relays operated in a push-pull arrangement. The circuit may be changed to connect the four sets of transfer contacts into a lattice configuration to supply battery reversals to the apparatus under test. This is used in testing core materials to eliminate residual effects and for polar relays and similar structures.

The electronic control circuits which apply or stop the relay winding currents will be described later.

Timing Control System

The timing control system consists of a frequency source, a pulse forming circuit, three binary-quinary ring counters in tandem, a time selection circuit, coincidence circuits, memory circuits, and three control circuits, one for each of the A, $B1$–$B2$ and C relay circuits. A block diagram of the system is shown in Fig. 11.

Oscillator. The frequency source is a bridge stabilized oscillator. This is compared to the Bell System standard frequency for calibration. The accuracy of measurement, both for magnitude and the time scale depends directly upon this oscillator. The magnitude error enters through equation (5) where the cycle time T is exactly the interval for 1000 cycles of the oscillator frequency by virtue of the 1000 discrete steps in the three decades. The time scale is determined by these same steps. Hence the accuracy and stability of the oscillator enters directly; 0.1 per cent can be realized easily. This is as good as necessary as it exceeds the dc instrument accuracy.

Pulse Shaper—The pulse shaper is shown in Fig. 12. It consists of an initial cathode coupled amplifier followed by three more direct coupled stages. The square wave output of the third stage is differentiated by a small condenser for voltage spire production. It is a Schmidt[3] type circuit designed by I. E. Wood.

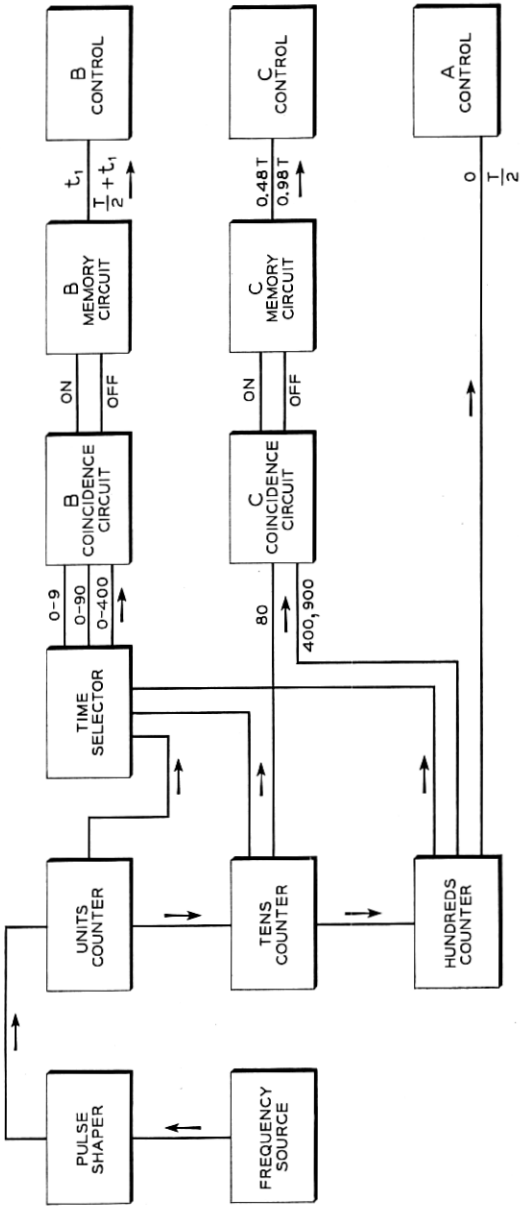

Fig. 11 — Block diagram of timing control system.

The differentiated output appears as a positive voltage impulse across the cathode resistor of a coupling tube, impressed on top of its normal dc bias due to current from the following quinary ring. The coupling circuit has the appearance of a cathode follower, but except during the short intervals of impulse transmission, the plate does not conduct. This lends itself to supplementary use of the rings as counter circuits. An on-off gate can be connected, as shown, to enable or disable the grid bias of this tube, without introducing any false starting or stopping counts.

Quinary-Binary Counters. The unit decade counter is shown in Fig. 13. It is a modification of Weissman's quinary-binary circuit[4] and was chosen because it provides simple two wire selection for the coincidence circuits. The principal modification consists of applying the shift pulses to the odd cathode lead rather than to a grid multiple, and using a direct coupled positive impulse for shifting.

The shaded tubes are non-conducting at 0 time and can be set in this condition by momentarily opening and then closing the reset key. The plate current from the right half of the zero tube passes through the cathode resistor of the output tube in the pulse shaper described above, and biases both tubes, the latter beyond cutoff. The plate currents from the other four tubes pass through the second cathode resistor having ¼ the resistance, developing the same bias.

A positive cathode impulse applied by the pulse shaper shifts the (0) tube from right to left half conduction. In shifting, the negative pulse from the prior non-conducting half of the zero tube cuts off the conducting half of the (1) tube, causing it also to shift. The shift of the (1) tube puts an aiding backward pulse into the (0) tube and a forward pulse into the (2) tube to keep it unchanged. Successive cathode impulses continue the ring stepping, the ring closing on itself after the fifth count. Thus the ability to shift properly depends solely upon the impulse waveform from the pulse shaper, which can be controlled independently of the ring circuit.

At the beginning of the fifth impulse, a square negative impulse is passed by the conducting half of the twin coupling diode to the (5) binary tube, causing it to shift. On the next round, the other half of the diode conducts, restoring the (5) tube. The twin diode behaves as an infinite capacitance in a circuit having zero time constant.

For each of ten successive impulses there is a different configuration of conducting tubes, and two wires, one to the quinary ring and the other to the binary tube, can identify when a selected state is reached by a coincidence circuit noting that a low voltage is present on each wire.

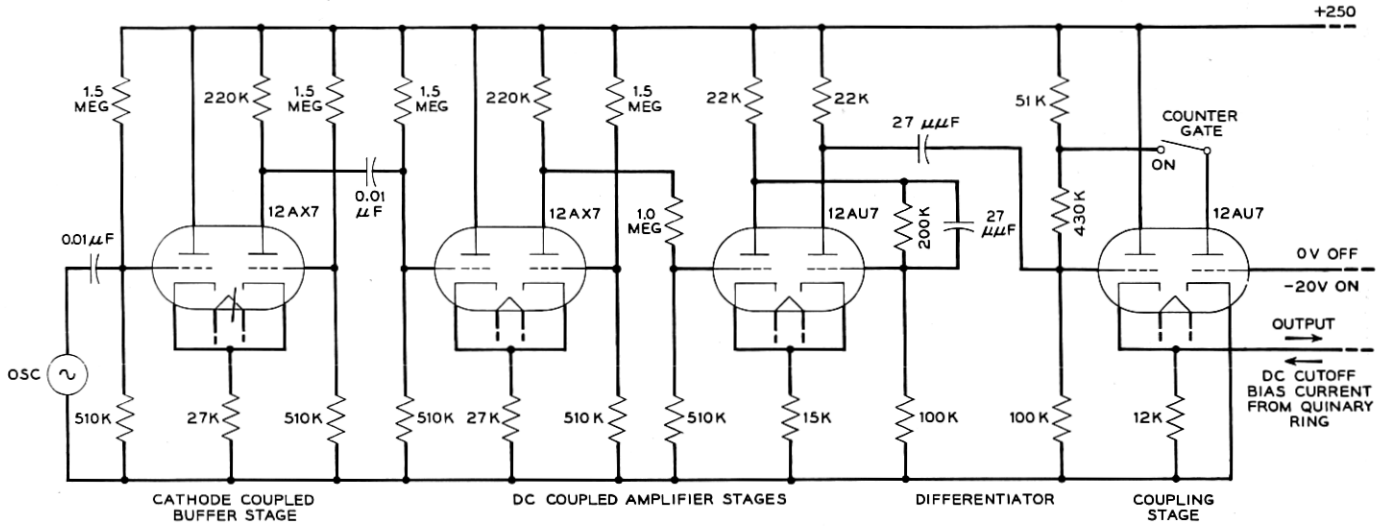

Fig. 12 — Schematic of pulse shaping circuit.

For the other nine configurations, one or the other of the wires will carry nearly the full battery voltage. The leads to the time selector switches are indicated by the arrows marked from 0 to 4, 5R and 5L, inclusive.

When the (5) tube reverts after the tenth impulse, its step plate voltage rise is differentiated by a small capacitor. This drives another pseudo cathode follower to shift the tens counter exactly as has been described for the units counter. For this tens ring, the take off leads to the time selector are identified as 00 to 50.

In a similar manner the hundreds counter leads are identified as 000 to 500.

Thus by exactly six wires, two for each decade, any cycle in 1000 can be selected, Note that for 0 and 500, needed for the *A* relay the (500) tube itself provides complete information. This eliminates the need for a coincidence and memory circuit for the *A* relay drive tube. Also by choosing 480 and 980 for the *C* relay, an abbreviated coincidence circuit can be used, as access to the units counter is not needed.

Neon lamps are provided as indicators for each ring to aid in circuit checking, trouble shooting, and as the counter indicator when used with the gate circuit.

The separation between successive time intervals which can be selected is one/one thousandths of one complete closure and open cycle, being 25 microseconds for a cycle time of 25 milliseconds, 100 microseconds for a cycle time of 100 milliseconds, etc. This is controlled by the discrete states of the counting rings used to generate the switching signals. This relation between the cycle time and the successive available time intervals is not a handicap because if the device is slow and a long cycle time has to be employed, it is slow because the flux buildup or decay is slow and hence closely spaced measurements are superfluous.

The maximum speed is 40 on-off cycles a second obtained with a 40-kc oscillator. The lowest speed is limited only by the ability of the vacuum tube filter to suppress instrument pointer vibration.

The counting ring system with its discrete steps precludes an automatically recording device as would be possible with a motor driven commutator and a gear driven take-off brush. However, the elimination of brush troubles is considered to be worth this sacrifice.

Time Selector. The time selection is controlled by two two-gang decade switches for the units and tens selections and one five position switch for the hundreds selection. The schematic is shown in Fig. 14. The dial positions are marked directly in time for a 10-kc oscillator, that is the units selector indicates one-tenth milliseconds, the tens milliseconds, and

the hundreds tens of milliseconds. For other oscillator frequencies the times indicated are scaled in proportion. Thus for a 40-kc oscillator, the indicated times are divided by 4 and the fine steps become 25 microseconds.

The start of the A cycle is marked by L500 and the stop by R500, the 500 tube itself serving as the memory circuit, and no coincidence circuit is needed.

The C cycle is wired permanently with a phase to close just before 500 and open just before 0. By choosing 480 and 980, access to the units decade is unnecessary and only four coincidence circuits are provided.

The start of the B cycle is marked by six coincidences, the end by five of these and the alternate connection to the 500 tube. The hundreds switch is simplified because the B relay always operates between 0 and 500 and releases between 500 and 1000. Therefore, the start and stop coincidence circuits can be wired permanently to the 500 tube and only

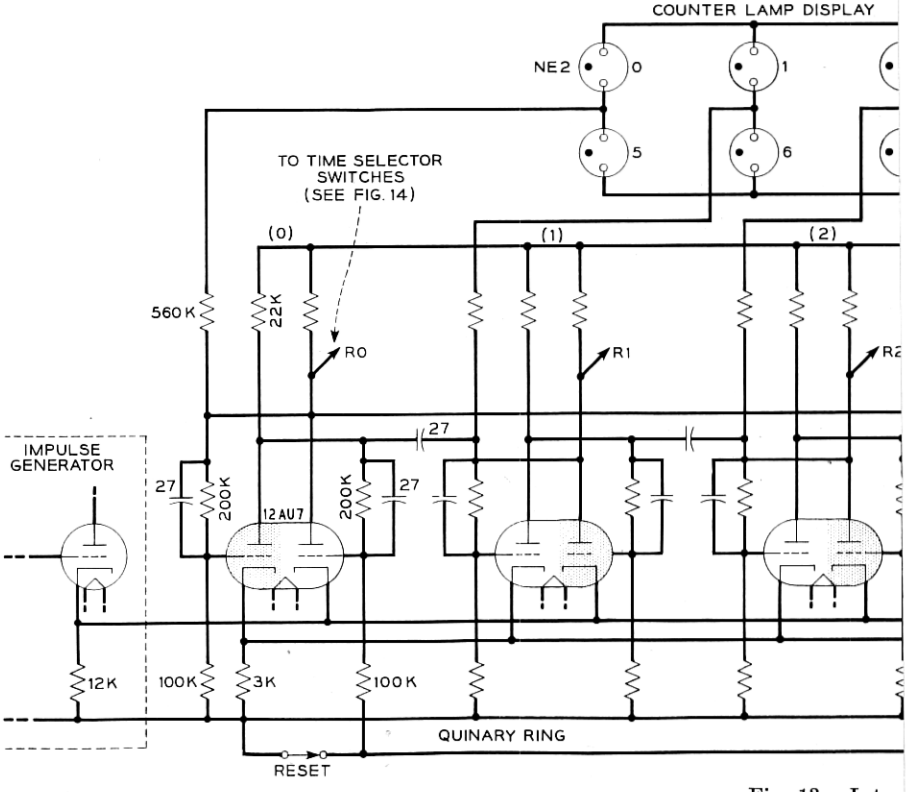

Fig. 13 —Inter

five switched wires are necessary. The change from flux rise to flux decay by another switch as shown in Fig. 10, converts the contact switching to provide the proper instrument closing time, with the time dials now reading time from the beginning of the open of the *A* circuit.

Coincidence Circuits. Each coincidence circuit consists of triodes, one for each marked wire. The circuit for the *B* cycle is shown in Fig. 15. Each selector switch wire connects to a grid, but all the cathodes of a set of coincidence tubes use a common cathode resistor. Except for the instant chosen, at least one coincidence tube has a high potential on its grid and the plate current through that tube holds the cathode resistor at a high potential. Only at the chosen time are all plates of the counter tubes conducting and therefore at a low potential. This abruptly drops the cathode potential of the coincidence circuit for one cycle of the oscillator, recurring every 1000 cycles. 500 cycles after each start pulse a similar stop

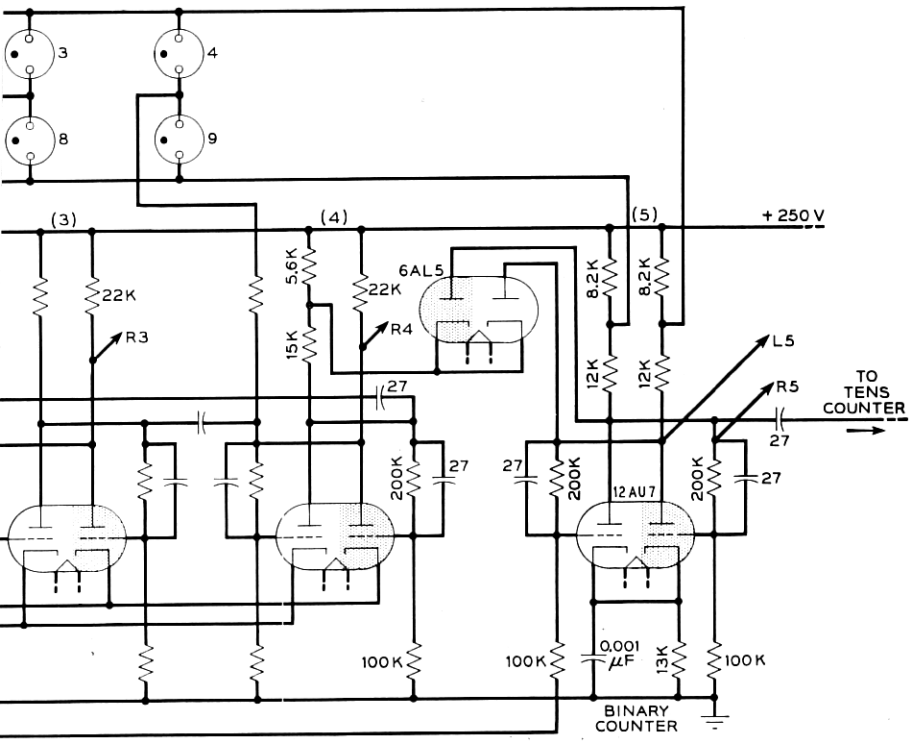

ner schematic.

pulse occurs in a duplicate set of coincidence tubes. These alternate pulses control the state of the memory circuit.

The *C* cycle coincidence circuits are similar except only four triodes are used for the start, and four for the stop pulses.

Memory and Relay Control Circuits. The memory and control circuits are shown in Fig. 16. The function of the bi-stable memory circuits is to accept the alternate start and stop pulses from the coincidence circuits, switch to the state representing the imposed condition, and hold it until the next successive imposed condition.

The function of the relay control circuits is to operate or release the relays under control of the memory circuits. The relay control circuits are direct coupled to the memory circuits and one or the other plate is cut-off by the grid bias condition imposed. The relays are in the plate circuits of the control tubes and either have full or no current applied. The operate and release times of the relays add a delay in the contact

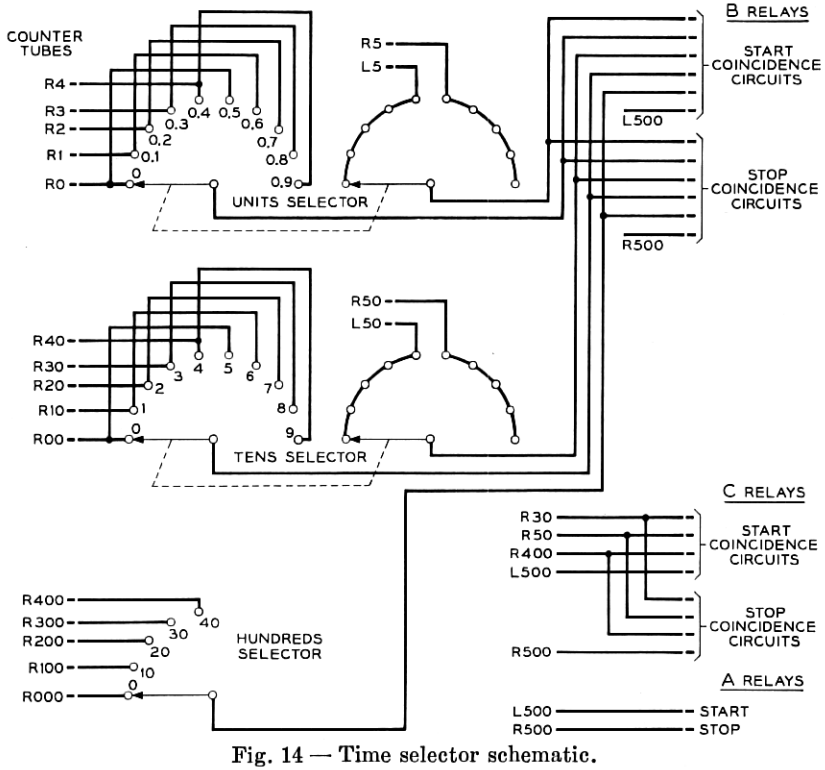

Fig. 14 — Time selector schematic.

actuation compared to the state of the memory tube. By making these small and equal, through selection of the relay design, the constant time lags do not alter the relative preset switching instants.

The relays are special mercury contact, single transfer, Western Electric 291-type. They have 38 gauge 1500 ohms, 14,600 turns windings and are adjusted to operate with 3.5 milliamperes and release with 2.0 milliamperes. The 5687 tubes switch from 0 current to 10 milliamperes through the relays. The release and operate times of the relays are about 1.3 milliseconds but as described earlier, are selectively adjusted to 1.5 milliseconds where necessary, by shunts such as those shown in Fig. 10.

The bi-stable memory circuits are switched at the grids through the twin diodes coupling the coincidence and memory circuits. While waiting for a shift pulse, the grid potential of the memory tube is lower than the cathode potential of the coincidence circuit, and the diode circuit therefore does not conduct. This is necessary because small voltage variations occur in the coincidence circuit cathode potential as the several tubes follow the decade counters. These small variations would shift the memory circuit falsely if directly connected. When the shift coincidence occurs, the cathode voltage drop is to a potential lower than that of the memory circuit grid and the conduction of the diode connects the two circuits. This negative impulse shifts the memory circuit. This drives the start grid to a new potential lower than that of the coincidence tubes cathodes, again cutting off the connection through the diode. When the coincidence cathode rises at the end of the shift pulse, the diode is even further cut off. The stop diode behaves in an exactly similar manner due to the symmetry of the circuits. The diodes thus afford a means of only momentarily making connections at the required instants, at all other times isolating the memory circuit from the remainder of the counting system.

Summary of Dynamic Fluxmeter Description

Up to this point, the circuit description has been concerned only with the dynamic fluxmeter. This circuit was designed and built first, and put into operation for dynamic current and flux studies of which one will be described later. About fifty standard type tubes in all are used, with good segregation of the circuit functions. This aids in localizing circuit troubles. Particularly useful is the neon indicator lamp display, also employed when the decade system, with the gate circuit, is adapted as a counter or time interval circuit.

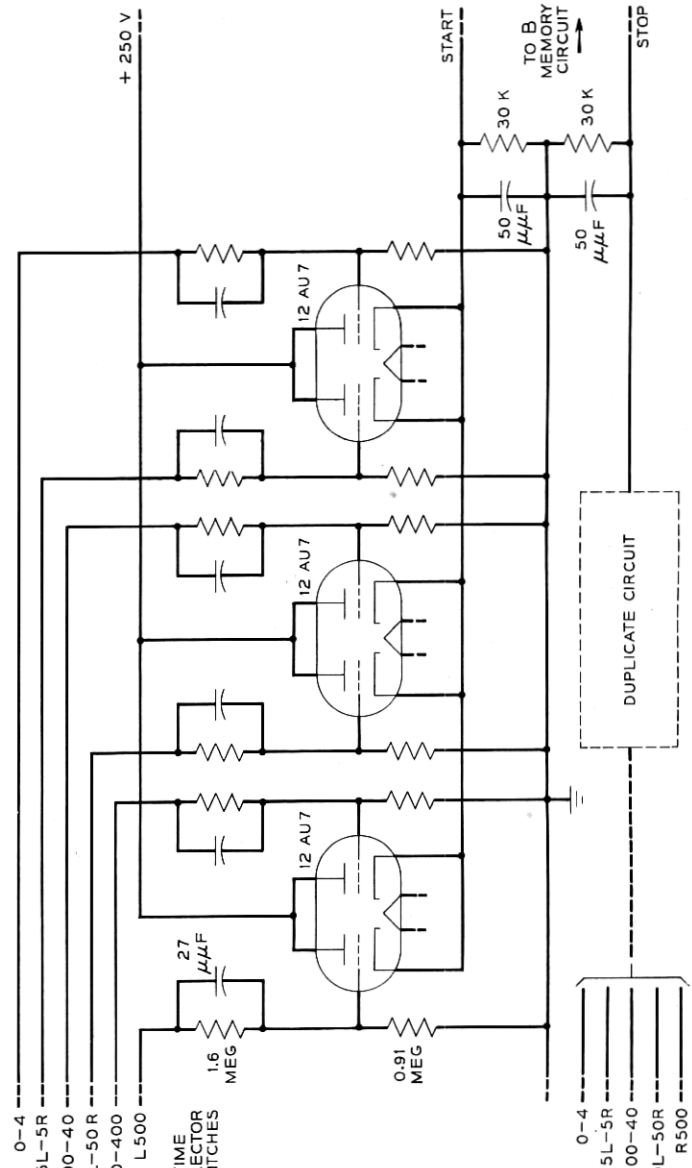

Fig. 15 — B-Cycle coincidence circuits.

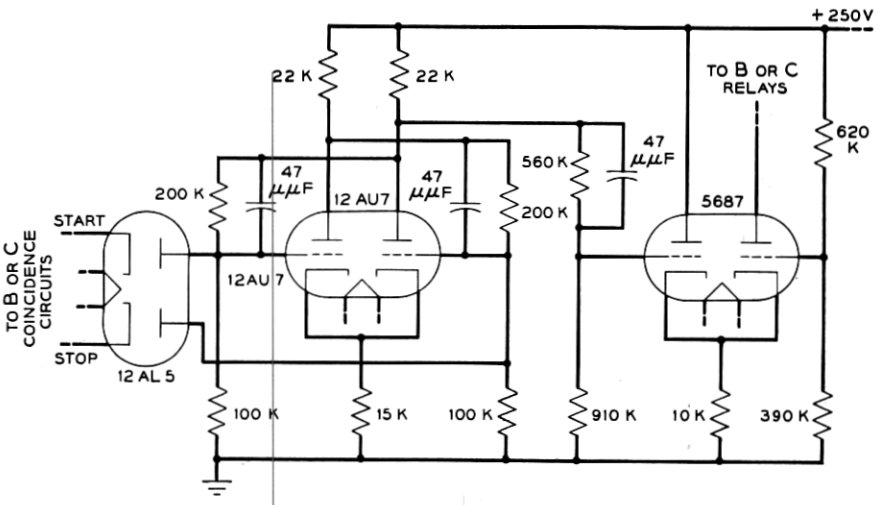

B OR C MEMORY AND RELAY CONTROL CIRCUIT

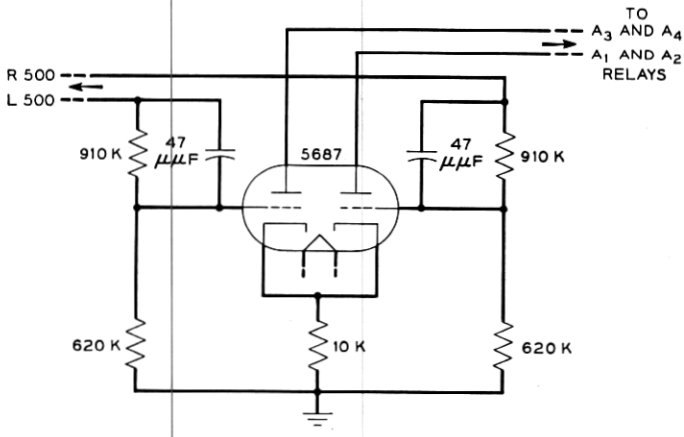

A RELAY CONTROL CIRCUIT

Fig. 16 — Memory and relay control circuits.

Part II — Displacement and Velocity Measuring System

The Optical System[1]

A block diagram of the displacement and velocity measuring system was shown as Fig. 4. As part of this figure, a geometric schematic of the optical part of the system is shown. Most of the features of the optical system are due to the advice and assistance of associates in these laboratories who were connected with the sound motion picture development. The fundamental design is similar to the film reproducing system with certain necessary changes in dimensions.

Referring to Fig. 4, the elements are the lamp, condensing lens, a slit, objective lenses, a vane on the part whose motion is to be studied, and a photocell. The lamp and the condensing lens are the same as are used in the film reproducer. The slit is the same except that its width has been increased to 0.005″ and a feature added permitting its length to be adjusted from zero to about 0.1″. The objective lenses are inexpensive Bausch and Lomb achromatic lenses. The second objective lens is interchangeable for different focal lengths, and may be moved back and forth in the supporting tube for precisely focusing the image of the slit on the moving vane.

The three lenses and slit are mounted in a tube fastened to the lamp housing which in turn is supported by adjustable supports mounted on a vertical stand. To the lamp housing support is also fastened the photocell container with its first amplifier tube.

A permalloy shield surrounds the photocell except for an opening for access of light which passes by the moving vane. The shield is provided to prevent the changing stray magnetic field from the nearby electromagnet under test from affecting the photocell current. This system can be moved in any of three directions for lining up with the vanes of the device being tested. The relay or structure being measured is not fastened to the optical system support, but is secured to another appropriate stand resting on the same laboratory bench.

This system may seem more complicated than necessary at first sight, but its advantage is that it provides a rectangular beam of light of constant width and adjustable length at the point being measured. The necessity of numerous light shields and screens is done away with, although it is advisable to throw a black cloth over the whole apparatus when once adjusted to keep out the overhead illumination.

The reason for this last is of interest. The fluxmeter timing is controlled by a stable oscillator. The 60-cycle power for the overhead lights is also

well controlled. The two systems therefore operate in substantially a synchronized fashion when convenient cycle times are chosen, such as 10 cycles per second. The overhead fluorescent lamps fluctuate in light intensity at 120 cycles per second, so that the contacts in the fluxmeter operate in synchronism with the fluctuations in light intensity. Any measurements made with overhead illumination getting into the photocell will therefore have a superimposed 120-cycle ripple. For the same reason extreme care has to be taken to avoid any 60-cycle pickup in the apparatus. The lamp and the heaters on the first amplifier tubes are supplied with well filtered dc and cannot be operated by ac. Noise not in synchronism with the contacts is of little importance, as the averaging of the meter cancels it. A comment on the linearity of the photocell should be made at this point. This system operates on a variable width, rather than a variable density basis. Consequently the linearity of the system depends upon the uniformity of emission of the photocell surface. This can be verified by moving a vane with a micrometer and recording the output of the amplifier with a precision dc voltmeter. If the relationship is not linear other photocells can be substituted until sufficient linearity is achieved.

Amplifier System

General. Fig. 4 showed the three dc amplifiers in block diagram form. These amplifiers have each been designed to operate with full internal gain from dc to 10,000 cycles. The external transfer characteristic of each is controlled by its input and feedback networks. The design of these networks provides ideal transfer characteristics from dc up to 10,000 cycles. At 10 kc, the frequency response deviates by less than 3 db from the ideal. This same frequency corresponds to a time constant of 16 microseconds. On a small signal basis, the fidelity of measurement therefore will extend to events occurring in times of the order of 16 microseconds.

A more serious limitation to the accuracy is the finite plate voltage available for the output amplifier which results in amplifier over loading on large peaks. As will be shown, this can delay the response of the meter to sudden velocity discontinuities.

The amplifiers have been designed to operate from two voltage supplies, plus and minus 250 volts. The −250 volts is a series regulated three stage circuit with an output impedance of less than 0.8 ohm at all frequencies. It also serves as the reference voltage for a three stage shunt regulated +250-volt supply. Keeping the magnitudes equal minimizes errors due to power supply voltage variations.

The photocell amplifier converts the current from the high impedance photocell into a proportional voltage, having an internal impedance of 10 ohms.

The following amplifier-differentiator has an internal gain of 80 db from dc to 10 kc. When used as a differentiator the rising external gain characteristic reaches 67 db at 10 kc.

The output amplifier also has an internal gain of 80 db from dc to 10 kc. The feedback network includes an equalizer to produce current, and hence flux, in the air core output transformer proportional to input voltage from dc to 10 kc. The inductance of the transformer, with constant applied ac voltage, would cause a 6 db per octave decrease in current above the frequency where its Q is unity. This is counteracted by designing the external amplifier gain to increase at 6 db per octave, starting at the same frequency. The output amplifier thus has the same characteristics as a differentiator at high frequencies and its external gain is 64 db at 10 kc.

The overall gain of the system, then, is 131 db at 10 kc. Stability has been obtained, even with this much overall amplification without resort to compartmentation. Each tube stage utilizes shielded turret construction, exposed interstage leads are very short and only the input grid leads are shielded because they connect to controls on the front panel. A box shield surrounds the gain selector and the displacement-velocity switch of the middle amplifier, the lowest level point on the main panel.

This system uses an electronic differentiator. Ordinarily in analogue computers, these are avoided because of the high-frequency noise introduced as a result of the attendant large amplification. In the present system, the averaging of the succession of impulses by the dc instrument minimizes this effect. With each cycle a discontinuous section of the noise is sampled, containing a dc component, but as these are random in sign, their average gives rise to no error.

The system is dc coupled up to the output transformer. Slow drifts, due to grid currents or other reasons, do not result in instrument current errors because of the differentiating action of the transformer. No actual dc source appears in the meter circuit itself. The only concern here is to maintain the amplifiers somewhere near their best operating point. Actually the main source of dc drift is the temperature coefficient of the photocell and the voltage stability of the lamp power supply.

Calibration. The calibration of the system starts with a static measurement of the total displacement of the reciprocating motion to be studied. This can be done using thickness gauges or a tool maker's microscope. Then the device is brought into alignment with the light beam and cycled

by the *A* contact. The cycle time is chosen for complete operation and the time selector is set for a time near the end of the operate interval. At this time the tested device is known to be at its maximum displacement, and the instrument reading, using the displacement connection, corresponds. A convenient instrument indication is obtained by adjustment of the amplifier gain controls. For instance if the displacement were 0.040″, an instrument reading of 200 microamperes could be used. At any other time, when the parts are in relative motion, the instantaneous displacement is read directly from the instrument using the same scale conversion factor.

The calibration for velocity measurements depends upon the displacement calibration and relationship between the input differentiating capacitor and the resistor it replaces. Once a displacement gain setting has been chosen, it must not be altered during the associated velocity measurements except by calibrated steps. The differentiating capacitor has been chosen so that an instrument displacement deflection, corresponding to a given number of thousandths of an inch, represents the same number in inches per second. For the example given above, a 200-microampere instrument reading would represent an instantaneous velocity of 40 inches per second, with a linear calibration for intermediate readings.

A plot of measured displacement and velocity for a fast wire spring relay shown in Fig. 21, will be described when system errors are considered.

Photocell and Impedance Transformer Amplifier. A schematic of the photocell and dc impendance transformer is shown in Fig. 17. The high vacuum photocell has an impedance of thousands of megohms and acts essentially as a constant current device, the current depending upon the instantaneous illumination. This current is connected to the grid of a series stabilized[5] twin triode amplifier tube, to which grid also is connected the current through the feedback resistor and a balancing current from the −250-volt power supply. The zero adjustment is made under quiescent conditions for the desired dc output voltage, there being, of course, essentially no dc current in the grid.

The Western Electric low grid current 420A input tube is stabilized both for heater voltage and plate potential. It provides a voltage amplification of exactly $\mu/2$ or 35, by virtue of the upper tube having an impedance exactly equal to that of the plate of the lower tube. This input tube is mounted immediately behind the photocell in the same shield.

The output from the first amplifier tube is connected through a double shielded cable to the output tube mounted on the main chassis. The 5687 twin triode output tube uses both halves as cathode followers, one

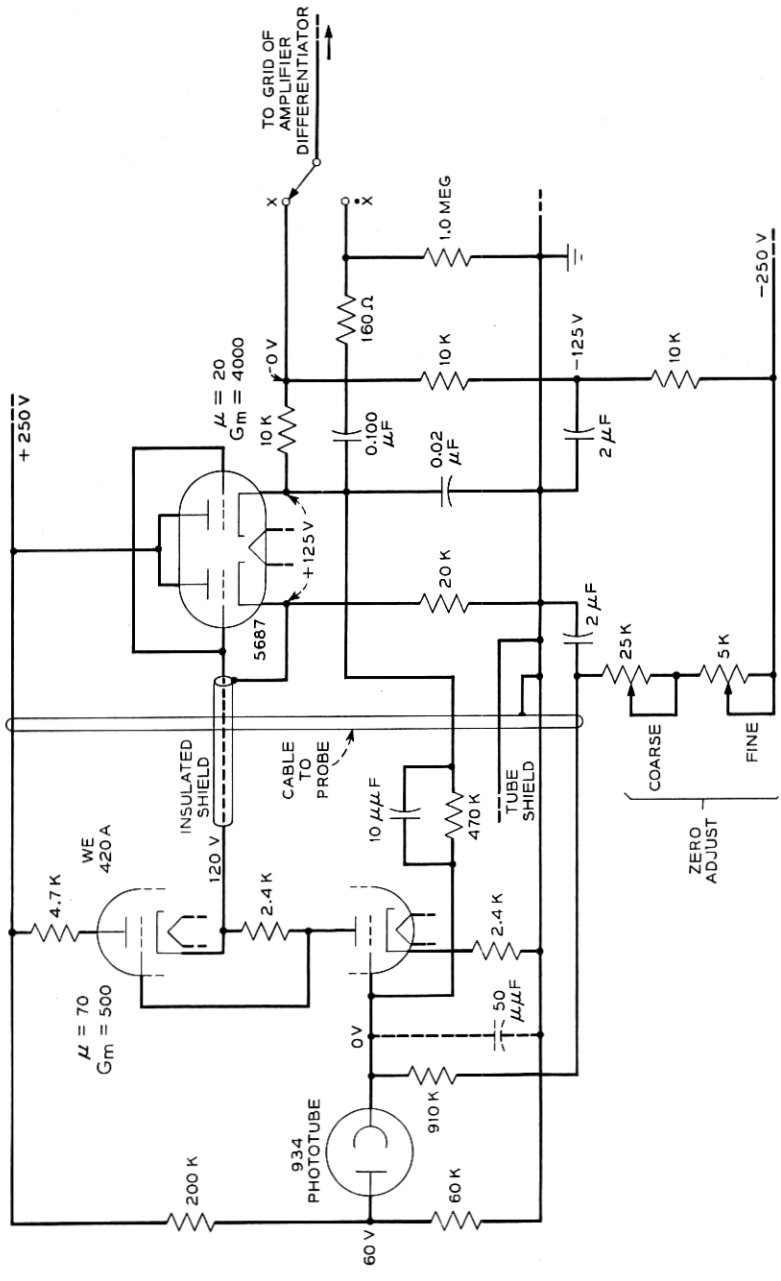

Fig. 17 — Schematic of photocell and DC impedance transformer.

to provide the output voltage and the other as a driver for the insulated inner shield to reduce the effective capacity to ground of the interstage cable connection. The cathode potential of the output tube is operated at exactly +125 volts, set by means of the zero adjustment previously described.

The input networks of the succeeding amplifier-differentiator are shown as part of this circuit as they provide the path for the output tube current and enter directly into the frequency response and loop gain cutoff design of this feedback amplifier. The dc grid voltage of the succeeding amplifier is 0, and this potential is found one-third the way down the cathode resistor which connects to the −250 volts. This point then provides the input to the following grid for displacement measurements and the input resistance for gain computations of the following amplifier is only this one-third part of the total cathode resistance or 10,000 ohms.

For velocity measurements, the succeeding grid is switched to the polystyrene differentiating capacitor whose grid side also is kept in readiness at 0 voltage by a grounded 1-megohm resistor.

For a change in current from the photocell due to a change in light, the feedback acts to supply an equal but opposing current from the output to keep the input grid nearly at its virtual ground potential. Thus the output voltage change E_s is given to a good approximation by the simple relation

$$E_s = \frac{I_s R_f \mu\beta}{1 - \mu\beta} \approx -I_s R_f , \tag{16}$$

where I_s = change in photocell current, R_f = feedback resistance, and $\mu\beta$ = loop gain.

A word about the differentiator connection is in order here. For this use, the cathode load approaches 160 ohms at high frequencies because the input grid of the next amplifier is a virtual ground point, and the load becomes equal to the phase shift controlling resistor in series with the 0.1 mf capacitor, the value of which will be discussed later. The impedance of the cathode follower without feedback is 250 ohms but this does not mean that it can be connected to a 250 ohm load and operated at the normal power output rating. The basic limitation for any tube is the allowable plate current change, regardless of the external load, consistent with never drawing grid current or being cutoff. For instance, in a cathode follower, if a load equal to 1/Gm is used, the small signal output voltage is only half of the applied grid voltage, a 6 db loss. Lower load resistances result in corresponding greater losses. In the present circuit, about an 8 db reduction in loop gain occurs at 10 kc

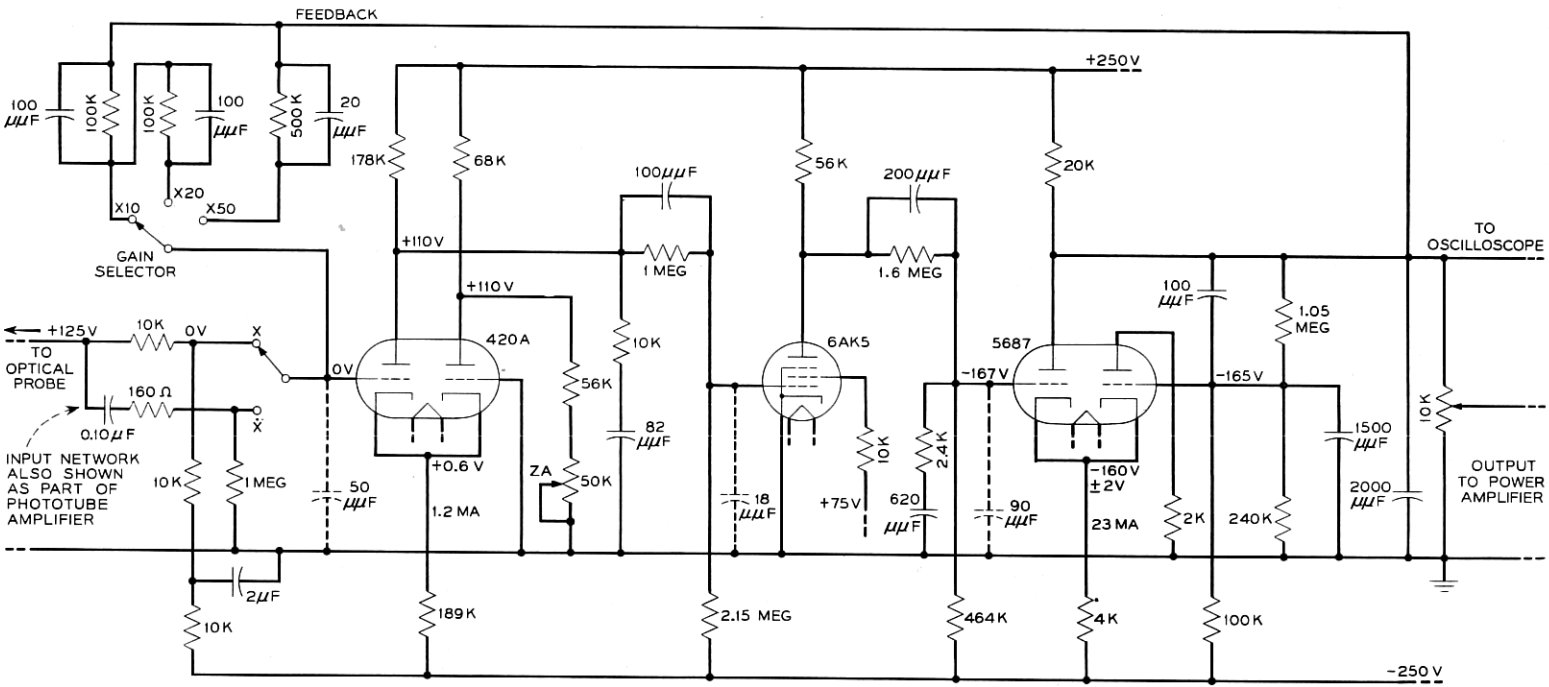

Fig. 18 — Amplifier-differentiator schematic.

leaving a net gain of about 22 db, including the 3 db effect of the input grid capacity.

Of equal concern is the reduced power handling capacity, but fortunately the energy in the frequency spectrum of the input signal diminishes rapidly with increasing frequency. A measure of this can be arrived at by the following analysis. The output voltage change for a motion of 0.040″ is about 0.1 volt. This total motion ordinarily never takes place in less than about 0.001 second, or a maximum rate of change of 100 volts per second. Now for a capacitive circuit

$$i = C \frac{dE}{dt} = 0.1 \times 10^{-6} \times 100 = 10 \text{ microamperes}, \qquad (17)$$

which is extremely small compared to the 12.5 milliamperes quiescent cathode current. Thus in choosing a vacuum tube to provide the desired amplifier output impedance characteristics, all other considerations have been cared for.

Amplifier-Differentiator. A schematic of the amplifier-differentiator is shown as Fig. 18. It has three stages, is direct coupled, and the quiescent output voltage is zero, set by the zero adjustment which controls the plate voltage of the inner tube of the input stage. The first stage is a conventional parallel stabilized circuit. It uses a high common cathode resistor to return the twin plate currents to the −250-volt supply. The first stage output is fractionated by an L pad to provide the proper dc bias for the second pentode stage. The output of the second stage is likewise fractionated for the dc bias of the final stage.

The third stage is a twin triode designed with an inside positive feedback loop. The two tubes have a common cathode resistor. After arbitrarily choosing one of the three grid resistors of the inside tube, the other two can be determined so that the proper quiescent bias and voltage changes result to make the plate current of the inner tube complement the plate current of the output triode itself. This maintains the total cathode current constant and establishes the cathodes as a virtual zero impedance to ground point. This realizes full gain from the output stage without another power supply. It also protects the triode from destruction if an accidental ground connection is made to the output.

The feedback circuit permits a choice of three values of resistances. The external amplification can be set at 10, 20, or 50. The maximum value of feedback resistance which can be used is determined by the value of the differentiating capacitor. It is set by the requirement that at least 10 db of loop gain remain at 10 kc.

It is now appropriate to discuss the scale factor for the differentiator

and to arrive at the value of capacitance to select. First we wish to measure reciprocating motions of the order of 0.050″ and actuating times of the order of 0.005 second. However, the motion takes place in the order of half the actuating time. Hence the average velocity will be of the order of 20 inches per second. An average numerical ratio of velocity to displacement then is 20 divided by 0.05, or 400. Remembering this is average and some part of the velocity will be higher the nearest decimal factor is 1000.

In this system, as a device being tested is a part of it, the instrument time scale necessarily is identical with real time, that is it cannot be "slowed down" for more accurate time settings, as can analogue computers.

Now once a convenient gain setting for displacement measurements has been determined, if a capacitor were substituted for the amplifier input resister, related by the equation $RC = 1$ second, C would be 100 *mf*, as $R = 10{,}000$ ohms. This would be a substitution where the scale reading for a given number of mil-inches would represent the same number of mil-inches per second. Fortunately, however, we wish rather to represent a much higher velocity of inches per second. This results if the capacitor is reduced by the same factor of 1000. The desired capacitance thus has a value of 0.10 *mf*. The type used is a stable, low soak polystyrene dielectric one having ½ per cent accuracy. In this amplifier the feedback and input resistors also must be of ½ per cent accuracy as upon these depend the calibration. The 10,000 ohms input resistor necessarily is a non-inductive wire wound type with a 10 watt rating, for stable performance with the actual 1.5 watts. The feedback resistors are of the deposited carbon type.

The remainder of the design now follows. To limit the differentiation action to a 10-kc range, a resistor in series with the 0.1-*mf* capacitor of 160 ohms is used. A transfer gain of 70 db, which is 10 db less than the internal gain of 80 db, is a voltage ratio of 3,160. Multiplying this by the input resistor value of 160 ohms yields 500,000 ohms as the maximum feedback resistance. Then as an amplifier with an input resistor of 10,000 ohms, the gain is 50. Resistances for lesser gains of 20 and 10 are scaled in proportion.

The linear output voltage range for this amplifier is ± 40 volts. This is much more than needed. For displacement measurements the maximum swing is about 5 volts. In the discussion, we found a maximum capacitor current of about 10 microamperes which also results in an output swing of 5 volts, during velocity measurements.

Output Amplifier. The schematic of the output amplifier is shown in Fig. 19. This amplifier also has three stages, the first two of which are

like those of the amplifier just described. Similar considerations for the overall design were used here and the loop gain cutoff control uses the same principles, modified to take account of the inductor load and its constant current feedback equilization.

The output tube is a 6L6 with an 874 voltage regulator tube in the cathode return to the −250 volts. The 6L6 is operated at 40 milliamperes, which is within the current rating of the 874. This stage was designed for the widest possible output voltage swing and for plate current cutoff independent of plate voltage, both characteristic of pentodes.

The transformer has a 900-cycle self resonance with its equivalent shunt capacitance. At higher frequencies it behaves as a capacitor as far as the tube and loop gain are concerned. Its Q is unity at 56 cycles.

The function of the output amplifier is to convert the input voltage signal into proportional current in the inductor. Constant voltage gain would not do this. For frequencies above 56 cycles, the current would drop at a 6 db per octave rate with increasing frequency, because of the reactance.

Note that if the voltage across the inductor rises with increasing frequency, then the current through the winding will be proportional to a constant input voltage regardless of the equivalent shunt capacitor. The capacitor will draw greatly increased current but as long as it is uniformly distributed, it will not affect the winding current itself. If series output feedback were used, the two currents could not be separated and a more complex equalizer would be necessary to provide the necessary frequency response. The choice of the value of inductance for the output transformer will be discussed after errors in the system have been considered.

The rising gain is produced by shaping the feedback, starting an insertion gain rise at 56 cycles with the 0.057-*mf* capacitor, and continuing to 10 kc. At this frequency the rising characteristic is discontinued by the 280-ohm series resistor, and the capacitors shunting the feedback resistors. Over the rising characteristic range the equilization introduces 90° adverse loop phase shift and above 900 cycles the output transformer adds another 90° phase shift. Thus from 900 cycles to 10 kc the amplifier just skirts being Nyquist stable.[6]

The internal gain of this amplifier is 80 db. At dc the external gain is 21 db. It rises to 67 db at 10 kc because of the feedback equilization.

Output Amplifier Square Wave Response

The square wave response of the output amplifier is shown in Fig. 20. Two effects are evident (1) a finite time for the major change to occur,

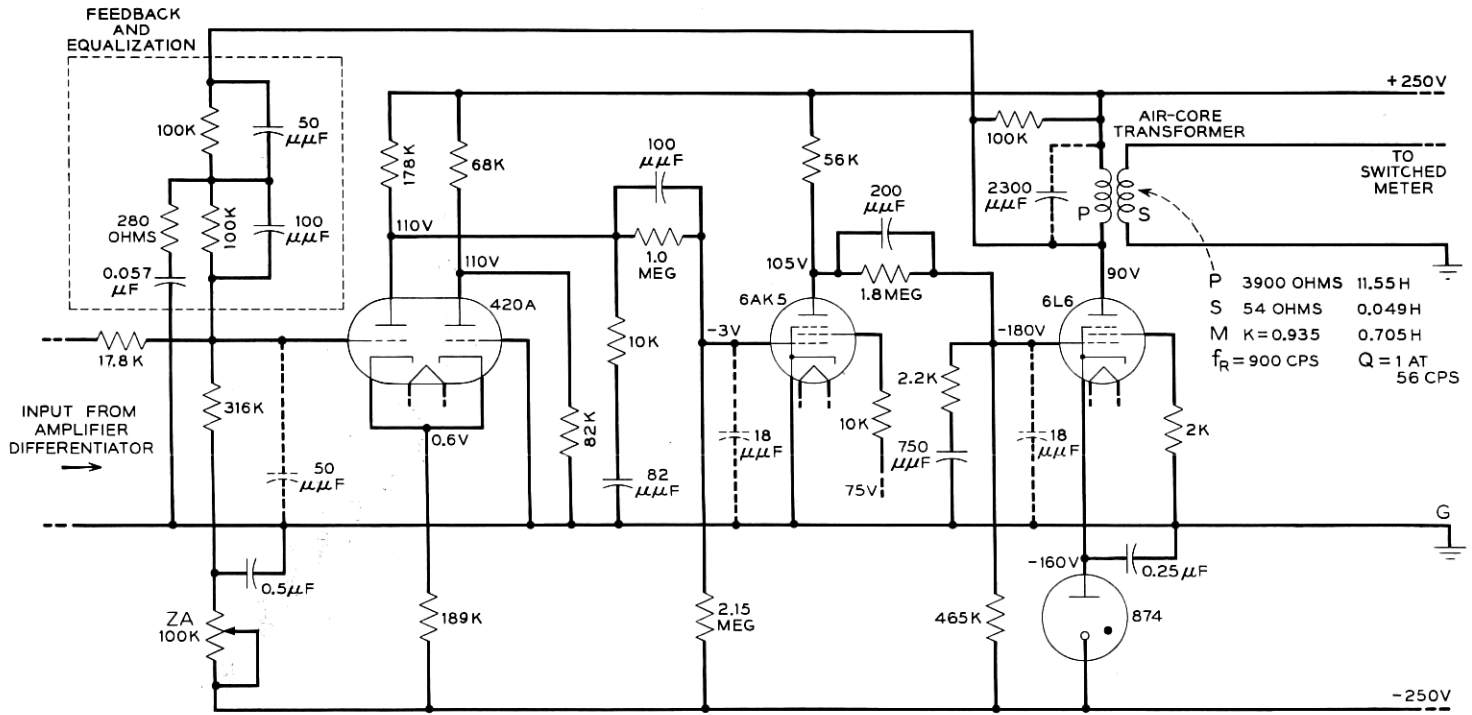

Fig. 19 — Output amplifier schematic.

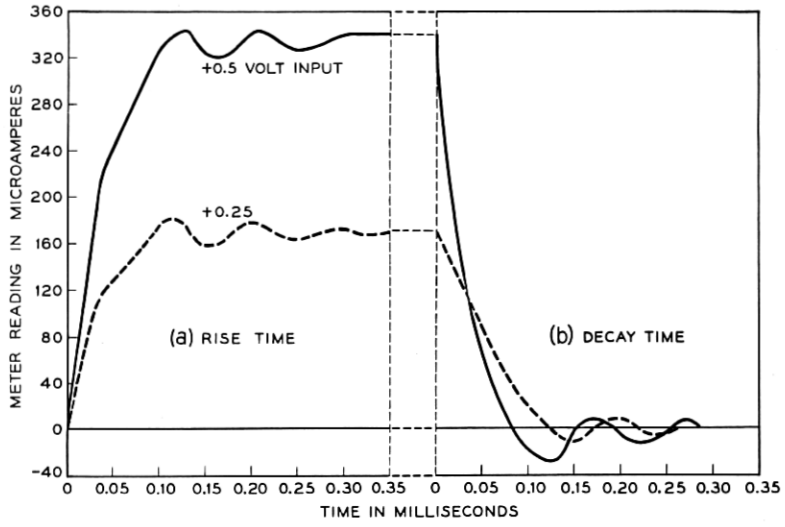

Fig. 20 — Output amplifier square wave response.

followed by (2) an oscillation caused by the frequency response of the amplifier deviating from the ideal for frequencies above 10 kc. The former effect is caused by the finite power supply voltages available in the final stage of the output amplifier.

The current in the primary of the output transformer represents the function being measured. If a step discontinuity occurs, as during velocity measurements, then the current suddenly has to be changed to a different value. The rate of change of an increase in current which can be developed is proportional to the power supply voltage, and hence is finite. For a decrease, the distributed capacitance of the winding and the shunting resistors delay the current decay. These result in a delayed transition from one condition to the other, occuring, from Fig. 20, in about 0.1 millisecond.

A discussion of the operating conditions of the system leads to a method of evaluating these forms of error and determining what limitations are imposed upon the use of the measured data. It will be shown that only immediately following velocity discontinuities are the data not usable. Displacement data are never in difficulty from an overload standpoint and fortunately we ordinarily are not too interested in velocities after impacts.

Discontinuity Errors Due to Overloading

The arbitrary gain setting for the output amplifier is chosen to provide about the full scale of 200 microamperes to represent the full displace-

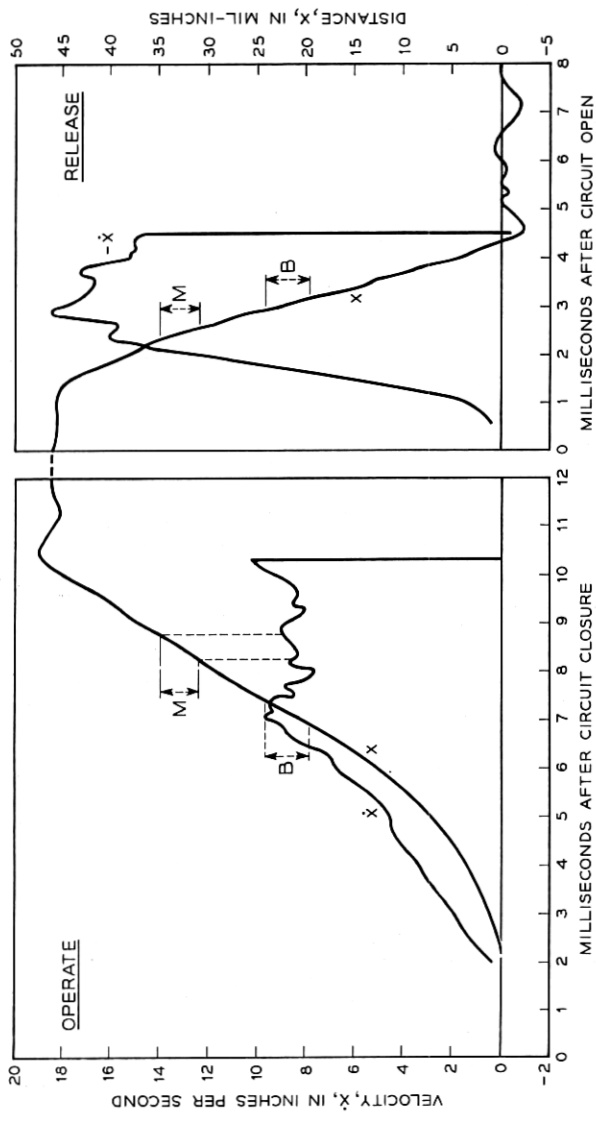

Fig. 21 — Displacement and velocity measurements of the AF-type relay. M — on operate, make contacts closed in this region, and on release, make contacts open in this region. B — on operate, break contacts open in this region, and on release, break contacts close in this region.

ment. The output transformer obeys equation (8), and its characteristics are tabulated on Figure 19. From this equation and a cycle time of 0.1 second we find that the change in plate current for a 0.705 henry mutual inductance amounts to 2.83 ma. The dc plate voltage change therefore is 11.32 volts and the corresponding input dc voltage is 1.0. These values are extremely small compared to the voltage swings available, but nevertheless the fact that the instantaneous voltage swings are finite imposes a limit to measurement of step discontinuities.

One direction of transformer current change is where we wish to decrease the current suddenly. The signal blocks the output tube and the transformer current decays through the equivalent of a 50,000-ohm shunt. The primary inductance is 11.5 henries and the time constant therefore is 0.23 millisecond. The quiescent current is 40 microamperes, so a drop of 2.8 microamperes, assuming the 6L6 blocks completely, would require at least 0.02 millisecond. This means that if there is a measurement discontinuity, the best the circuit can do is to respond as the first part of an exponential over at least this time interval, rather than abruptly. This is shown in Fig. 20, where the indicated time actually approaches 0.1 millisecond. This extension evidently is contributed to by the distributed capacitance of the winding.

The current rise case is about as favorable. The current rise rate is limited by Lenz's law to a maximum value of

$$\frac{di}{dt} = \frac{E}{L} = \frac{265V}{11.5H} = 23 \text{ ma/ms.} \tag{18}$$

A change of 2.83 microamperes therefore requires at least 0.12 millisecond. This is also shown in Fig. 20.

The foregoing discussion has been directed toward establishing that the initial delays of Fig. 20 are entirely overload effects and not a frequency response effect. Thus if required rates of change during a test do not exceed the available rate, then no error of this type will occur.

Fig. 21 is a measurement of a fast relay. One curve designated x, is the displacement versus time. The other curve marked $\dot{x}$, is the velocity. In neither the displacement curve nor the velocity curve before impact, do the rates approach the overload condition.

The impacts are shown on the velocity curve to have the extreme rate of change. Such abrupt curves cannot be taken as being literally true. Following such abrupt changes the 10-kc oscillations also are found, but have not been drawn as they have to be discarded.

Discontinuity Errors Due to Averaging

Another effect acts to limit the sharpness of measurement when discontinuities occur. This is due to variations in successive operations of the device being tested. Obviously, if the actuation time varies over a range of ± 0.1 milliseconds, then any device such as the present one which measures by averaging many measurements, will not measure accurately in the close vicinity of such a discontinuity.

For a displacement measurement made at the average time of armature impact, part of the measurements will be before impact, the others after. The meter therefore will register too small a displacement. For another measurement a short time earlier or later than the impact part will be before and part after the average instantaneous displacement but the instrument average will still be good because the function now is smooth. The only displacement error then is just at impact and when the data are plotted, appears as a rounding of the curve. A good correction can be made merely by continuing the adjacent slopes to a sharp intersection.

A more striking effect is observed for velocity. At the moment of armature impact against core, the velocity drops suddenly from maximum to zero. The indication shown by the instrument then for this averaging type error is just half the final velocity. Another measurement made a short time earlier is good and the slope from that region can be extrapolated to the instant of the half velocity indication as the plot for the true velocity.

Choice of Output Transformer Inductance

The output transformer primary inductance is a compromise between output amplifier gain limitation due to equivalent shunt capacity of the inductor and the lowest desired cycle time. It was shown above that at at 0.1 second cycle time only 1 volt is needed for a full scale deflection whereas 5 volts is available. As the instrument current is inversely proportional to the cycle time, 1.0-second cycle time will provide about half scale. The 11.5H chosen then, just barely covers the timing range of present interest. The impedance of the equivalent shunt capacitor at 10 kc is approximately equal in magnitude to the transformer dc resistance, and full internal gain is available over the operating frequency band.

The delay time is not altered by a change in inductance. For instance, if the inductance were halved the rate of current rise would be doubled but twice the change would be necessary for the same instrument deflection. The same result can be had merely by reducing the gain by one-half.

If longer cycle times were needed without the short times of present interest, the inductance could be appropriately increased, and the amplifier bandwidths correspondingly decreased, without loss of accuracy.

Summary of Amplifier Discussion

The foregoing discussion of the amplifiers covers the design considerations, the required frequency responses, and errors because of divergence from the ideal. For displacement measurements, all events occur in intervals greater than the minimum which the amplifiers can follow. This is also true of velocity measurements as regards the photocell amplifier and differentiator. The output amplifier does overload momentarily at jump discontinuities of velocity, and in the time vicinity following such events is in error.

Another type of error caused by variations in successive operations of the device being tested can be corrected by use of the measured rates just before and after the discontinuity.

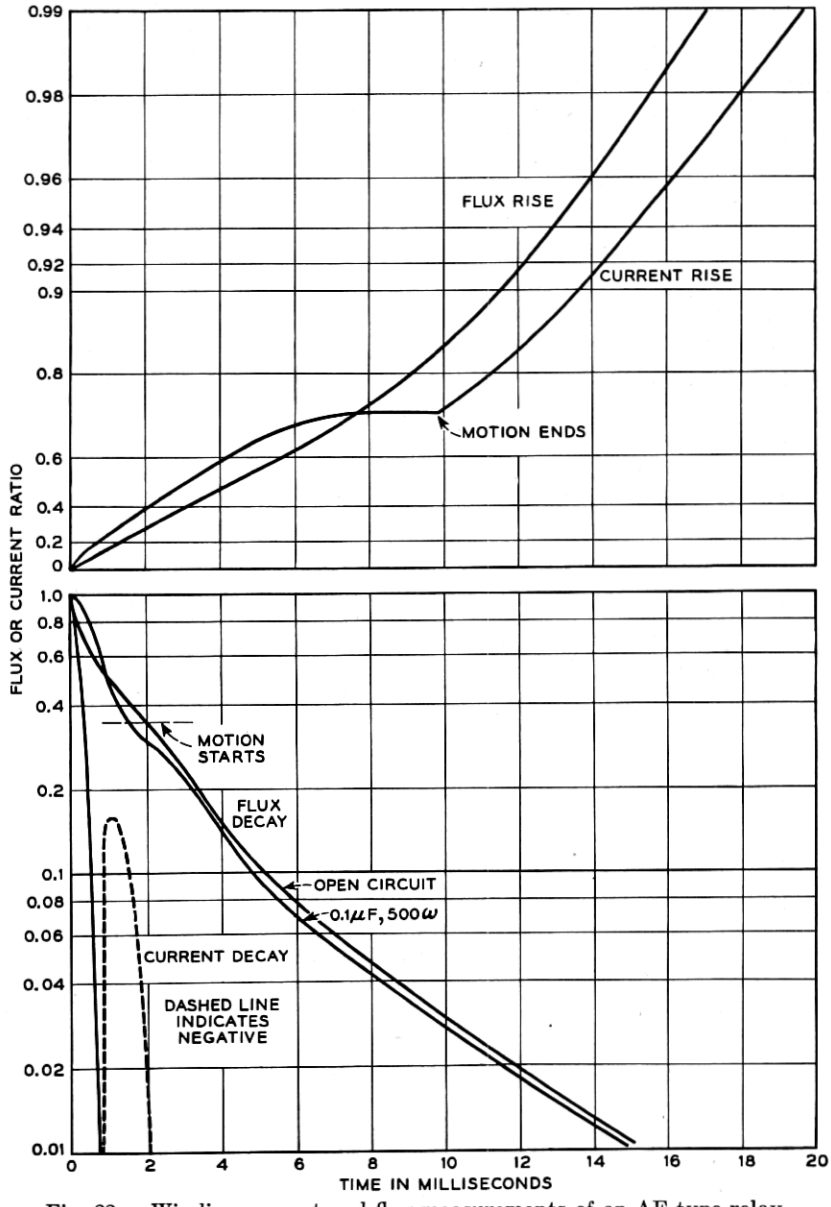

Fig. 22 — Winding current and flux measurements of an AF-type relay.

Part III — Applications

NEED FOR DYNAMIC FLUX MEASUREMENTS

The results of an experimental determination of dynamic flux rise and decay in solid core electromagnets are of general interest. Analytical solutions have been obtained for linear infinitely long rods or toroidal shaped structures where geometric simplicity exists. These solutions are in infinite series form. These solutions show that an elementary perfect representation can not be expected, even for these simple cases. Furthermore, an electromagnet has other factors which make any attempt at an analytic solution impractical. Some of these are:

(a) The magnetic material is non-linear.

(b) The flux density is non-uniform because of leakage flux.

(c) The varying geometry of the magnetic parts, including the necessary gaps, make the boundary value problems unmanageable.

(d) Motion of the armature during operate and release.

These all lead to the conclusion that a quick and accurate method of measuring dynamic flux changes is necessary for fundamental studies of the dynamic behavior of electromagnets.

As an example, Fig. 22 shows dynamic flux and current rise and decay measurements made on the same relay used for the dynamic motion studies. These data are plotted on semi-log graph paper as on such a plot an exponential curve becomes a straight line. The current rise curve shows the dip due to armature motion, ending abruptly when the motion is completed. The flux rise curve starts off nearly as an exponential but rises more rapidly after armature motion starts.

Two decay curves are shown, one with an open circuit and one with a contact protection network. Associated with the latter is the winding current which flows through the network. In the open circuit case, even without the effect of armature motion, the flux decay is not exponential. The flux decay with the network has a somewhat oscillatory shape about the open circuit curve. The current itself does complete one heavily damped cycle. The reversed current flow is shown as a dashed curve.

The decrease in flux after a short interval compared to the open circuit case, demonstrates that such a network can decrease the release time as well as afford contact protection.

For more fundamental studies, it is better to study flux behavior with the armature held fixed and avoid the motional effects.

DYNAMIC FLUX DECAY AND DEFINITION OF EQUIVALENT CORE CONDUCTANCE

Fig. 23 shows another measured flux decay curve with the armature locked in the operated position. Also shown are two one-term exponential

equations for comparison. For such an open circuit decay curve, the flux does not abruptly drop to zero because of induced core eddy currents. The analysis of these data thus partly resolves into the determination of some method for conveniently representing the eddy current effects.

NEW APPROXIMATE FLUX DECAY EQUATION

For a first approximation, use can be made of linear circuit theory. Assuming the core behaves as a coupled single turn of conductance G_e and inductance L_1, and defining the core time constant as:

$$t_e = L_1 G_e, \tag{18}$$

the flux decay equation is the well known solution:

$$\frac{\varphi}{\Phi} = e^{-t/t_e} \qquad t \geqslant 0. \tag{19}$$

It is clear that the dynamic flux decay cannot be represented by the above exponential equation, which has been drawn on Fig. 23 as the upper straight line.

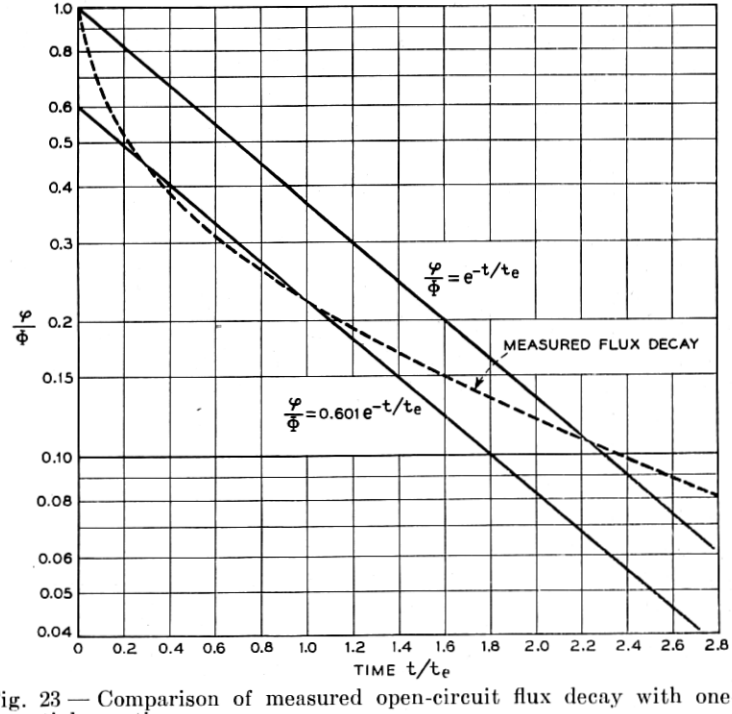

Fig. 23 — Comparison of measured open-circuit flux decay with one-term exponential equations.

The true decay curve has an initial steep slope followed by continuous curvature. A better approximation is to stipulate an initial jump discontinuity. A good fit to the flux range in which release of electromagnets occurs, shown by the lower straight line, is

$$\frac{\varphi}{\Phi} = .601e^{-t/t_e} \qquad t \geqslant 0. \tag{20}$$

This discontinuity of flux in the first approximation is just the reverse of the continuity of flux concept usually used. Of course, no actual discontinuity occurs, as shown by the true decay curve. The failure of any single exponential equation to represent the true curve merely makes clear the fact that the behavior of the core is not that of a single coupled turn, but rather is that of an infinite line. Bozorth[7] gives the intercept as 0.691 for the linear case, which does not represent the continuously curving decay which actually occurs.

The chosen intercept of the first approximation curve at $t = 0$ is admittedly somewhat arbitrary. It was arrived at in a broader study including flux rise curves. Accepting this equation, a convenient determination of t_e can be made similar to that for exponentials. If t is set equal to t_e, then

$$\left.\frac{\varphi}{\Phi}\right|_{t=t_e} = 0.221. \tag{21}$$

Thus, after measuring a dynamic flux decay curve, the time can be determined for which the above ratio obtains. This directly is t_e. From linear circuit theory and Lenz's Law, the inductance for one turn is:

$$L_1 = \frac{\Phi}{NI}, \tag{22}$$

whence G_e can be determined.

Now because of magnetic saturation and the shape of the hysteresis loop, the values will depend upon the particular final ampere turns (NI) used in the experiment. For uniqueness and uniformity in rating electromagnets for comparison purposes, the particular set chosen is that for which L_1 is a maximum. For comprehensive operating studies, measurements of course have to be made under the actual conditions of interest. Except for rating purposes, t_e is not ordinarily split up into components.

Thus, while the rated value of G_e for a particular electromagnet has the dimensions of conductance, it includes other factors as well. Some are: (a) Core material conductivity, (b) Magnetic non-linearity, (c) Shape of the hysteresis loop, (d) Non-uniform flux distribution, (e) Effect of pole

face and other air gaps, and (f) Decay of leakage field. It, therefore, also has the nature of a mop-up factor in which is included other effects not explicitly covered in the elementary analysis.

The above discussion has been directed toward establishing an easily determined core time constant having characteristics useful for rating purposes, and demonstrating that the distributed nature of the core eddy currents precludes an accurate representation of the core as a single coupled turn.

Open circuit flux decay measurements of round and rectangular solid core electromagnets of magnetic iron, 1 per cent silicon iron, and 45 per cent permalloy all are accurately represented by the measured flux decay curve of Fig. 23, after establishing appropriate values for G_e and L_1 in each case.

DYNAMIC FLUX RISE

Dynamic flux rise curves, measured with the relay armatures blocked open, are shown in Fig. 24. A family of curves, is needed because of the added variable of the winding. The value of t_e is determined by the method just described, except that the armature is held open, resulting primarily in a new and lower value of L_1. The winding may be characterized by its coil constant:

$$G_c = N^2/R,$$

where N = number of turns, and R = dc resistance of winding circuit. These curves are a composite of measurements on many structures and fit all data to within a few per cent.

An empirical closed form expression has been determined which fits these data, and in fact was used to compute these curves. However, once the curves have been plotted there is no further need for the rather complicated expression. Any particular rise curve desired can be interpolated from the drawing.

These curves again show, with windings of relatively low coil constants, a divergence of the dynamic flux rise from being a straight line. The particular curve $G_c/G_e = 0$ actually is a decay curve because such a rise measurement would involve the use of both an infinite voltage battery and an infinite resistance winding. Now for this case, as well as for all the others, the rise and decay curves differ because of the shape of the hysteresis loop, the decay curve persisting longer. This effect is most evident for the last few per cent of the flux change. However, the differences are small on a full range basis. The curves shown near $G_c = 0$ are

a compromise for this effect. Actually the rise curves do not cross, but they do approach each other.

Coil to core constant ratios now in use range from 2 upwards, the case of 2 being the best condition for 25 watts power. An examination of this particular curve shows some curvature for small times. This effect of an initial increased rate of rise reduces the operate time of an electromagnet, and is automatically taken advantage of in the experimental design of windings.

With a winding as part of the system, an elementary consideration shows why this curvature exists. This follows from

$$N \frac{d\varphi}{dt} = E - iR, \tag{23}$$

where: N = number of winding turns, E = applied battery voltage, R = resistance of winding, i = instantaneous current, and φ = instantaneous flux. This equation is exact and holds whether or not there are eddy currents. At the instant of circuit closure there are no winding or eddy currents (because of leakage inductances if for no other reason) and the initial rate of flux rise is dependent only upon the number of turns and the applied voltage. After a transition interval, the eddy currents become effective and slow down the rate of flux rise. For any given total flux, the time required, therefore, is less than that given by the well known equation:

$$\frac{\varphi}{\Phi} = 1 - e^{-t/L_1(G_e+G_c)}. \tag{24}$$

However, for large coil constants where G_c predominates the effect diminishes and the above equation is an excellent representation and desirable for its simplicity.

NEW FIRST APPROXIMATION FLUX RISE EQUATION

Returning to Fig. 24, while the effect we have been discussing is all important for open circuit flux decay, practical coil constants at present do not have ratios to the core constant much below 2. These curves do not diverge greatly from straight lines on this plot. Can a minor correction term be made a part of the simple equation heretofore used which will retain its simplicity and extend its accuracy to windings now used?

One such equation is

$$\frac{\varphi}{\Phi} = 1 - e^{-t/L_1(G_c+G_e e^{-G_e/G_c})}, \tag{25}$$

where Φ is the final flux. This may also be written in integral form as

$$t = (G_c + G_e e^{-G_e/G_c}) \int_0^{\varphi} \frac{d\varphi}{NI - Ni}. \tag{26}$$

The change is the introduction of the exponential modifying the core constant G_e.

Fig. 25 shows comparisons of curves for four different coil to core constant ratios. In each case, the actual flux rise, the older equation, and the new first approximation are shown.

For large coils (as an example on Fig. 25, $G_c/G_e = 10$) the actual flux rise is well represented by either expression, their accuracy being within 1 per cent.

For very small coils (on Fig. 25, $G_c/G_e = 0.5$) it is clear that the older representation is never a good approximation of actual flux rise. The new approximation represents the start of the dynamic flux rise quite well, but is not accurate for the second half. However no single exponential

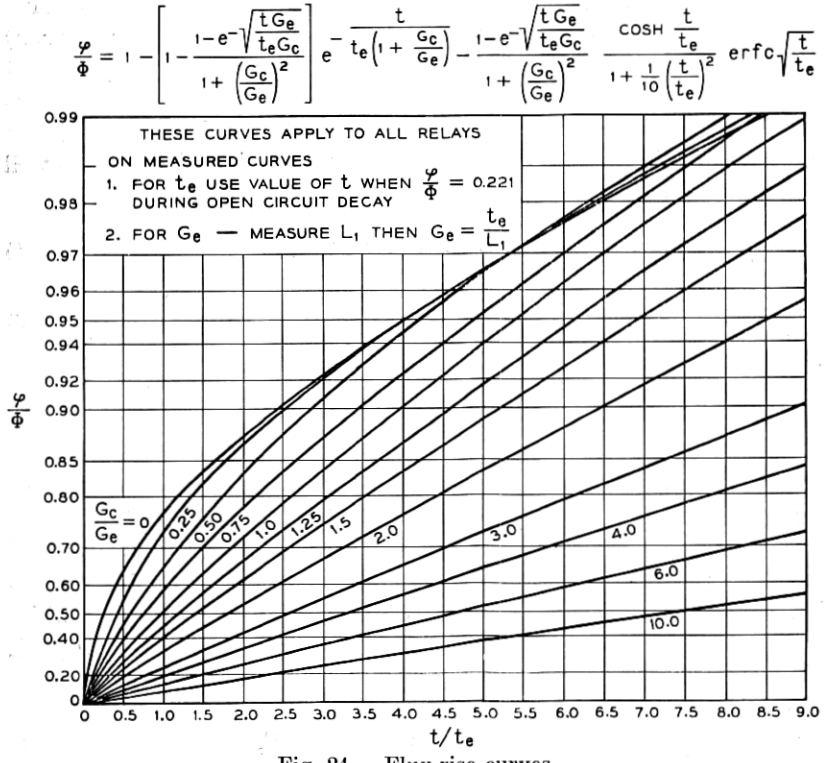

Fig. 24 — Flux rise curves.

equation can represent the actual rise when the plot is as curved as this one is. The best that can be done is to approximate the more important initial part with a straight line, and in this sense the new approximation shows a good fit.

A typical speed relay will have a value of G_c/G_e around 2 and the range from 1 to 10 covers all relays in this class. For a ratio of 2, the new representation of flux rise is within 2 per cent of the actual rise, as opposed to about 5 per cent with the earlier equation. For the ratio of 1, the accuracies are 4 per cent and 11 per cent respectively.

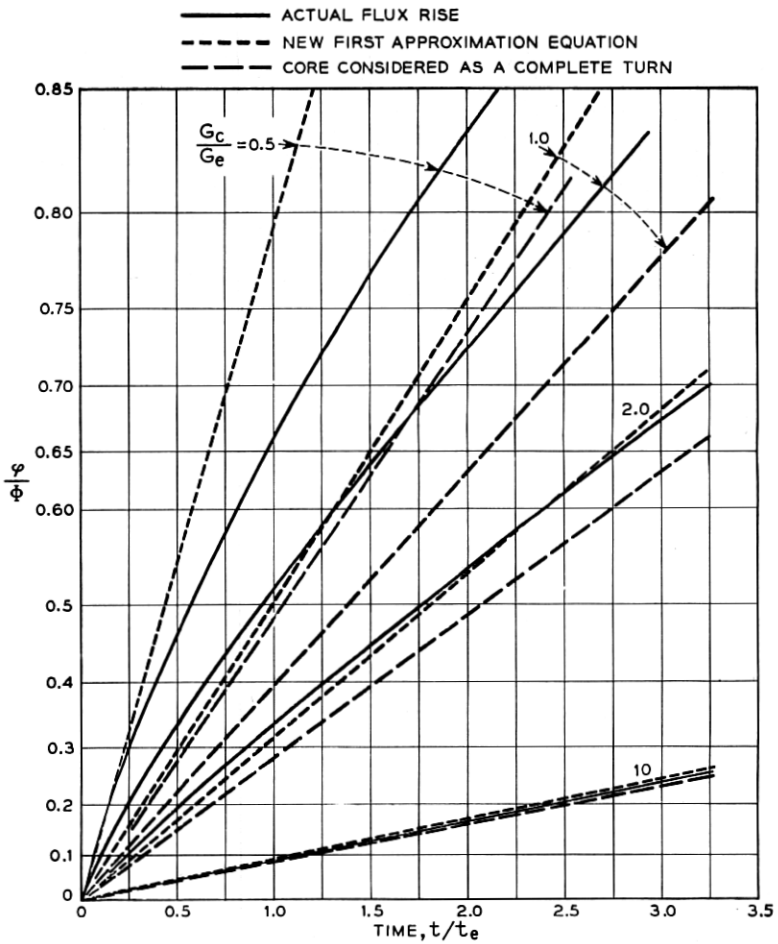

Fig. 25 — Comparisons of equations for flux rise.

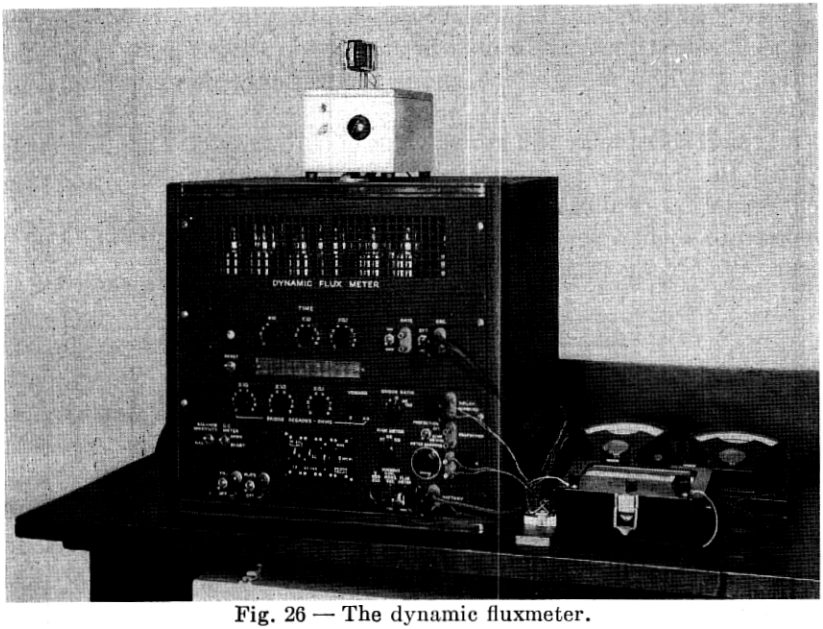

Fig. 26 — The dynamic fluxmeter.

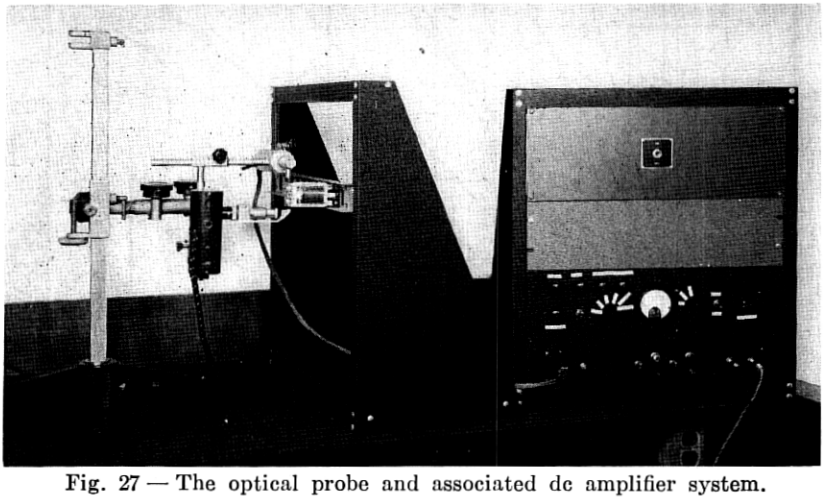

Fig. 27 — The optical probe and associated dc amplifier system.

Thus we have shown the new expression more accurately represents the eddy current effect on the initial flux rise for speed coils, and for most relays the overall accuracy will be within 2 per cent, and all relays should be within 4 per cent, an error reduction of about two-thirds compared to the older approximation.

EQUIPMENT

The dynamic fluxmeter is shown in Fig. 26. Two panels, each with a subchassis attached, comprise the set. The dc instrument and a supplementary voltmeter and ammeter are on the bench beside the cabinet. The upper panel contains the timing system, with the time selection controls. The lower panel includes the power supply and the test relay circuit controls, including the mercury contact relays. The control keys arrange the test relay circuit for any test condition.

The optical probe, a test relay, and the dc amplifier system are shown from left to right in Fig. 27. The photocell is in the shielded container above the relay, with the lamp and lens system below. A right angle prism turns the light beam into the vertical, to pass between the vanes on the relay.

The upper panel of the bench rack is the −250-volt supply. The lower panel includes the +250-volt supply, the three dc amplifiers and the magnetically shielded air-core output transformer. Its secondary is connected to the fluxmeter through a shielded cable. The controls are for zero setting the dc amplifiers, for selecting the amplifier gain and whether a displacement or velocity measurement is to be made.

REFERENCES

1. E. L. Norton, Dynamic Measurements on Electromagnetic Devices, A.I.E.E. Trans., **64,** p. 151, April, 1945.
2. Keister, Ritchie and Washburn, *The Design of Switching Circuits*, D. Van Nostrand, 1951.
3. Otto Schmidt, Thermionic Trigger, J. Scientific Instr., **15,** p. 24, 1938.
4. Richard Weissman, Stable Ten-Light Decade Scaler, Electronics, **22,** May, 1949.
5. M. Artzt, Survey of DC Amplifiers, Electronics, Aug. 1945.
6. Bode, *Network Analysis and Feedback Amplifier Design*, D. Van Nostrand 1945, p. 162.
7. R. M. Bozorth, *Ferromagnetism*, D. Van Nostrand, 1951, Chapter 17.